Electronic Thesis and Dissertation Repository

8-15-2017 12:00 AM

Contribution of Activating Transcription Factor 3 to development of acinar-to-ductal cell metaplasia

Jelena Toma, *The University of Western Ontario*

Supervisor: Dr. Christopher Pin, *The University of Western Ontario*
A thesis submitted in partial fulfillment of the requirements for the Master of Science degree in Physiology
© Jelena Toma 2017

Recommended Citation

Abstract

Pancreatic ductal adenocarcinoma (PDAC) is the third leading cause of cancer death in North America. The highest risk factor for PDAC is recurrent pancreatitis. While the link between PDAC and pancreatitis is unknown, de-differentiation of acinar cells is common to both diseases. Our lab has shown that Activating Transcription Factor 3 (ATF3), a factor upregulated during pancreatic injury, contributes to the development of acinar-to-ductal cell metaplasia (ADM), a precursor phenotype of PDAC. The goal of this study was to identify how ATF3 contributes to ADM. I hypothesize that ATF3 regulates acinar gene expression promoting ADM. We observed decreased ADM development in $Atf3^{-/-}$ acinar cultures, along with expression changes in differentiation genes and ADM promoting pathways (EGFR) *in vivo*. Assessment following chronic injury indicated absence of ATF3 resulted in decreased tissue damage. These results suggest a novel mechanism where ATF3 promotes ADM through loss of the mature acinar cell phenotype.

Keywords

Co-Authorship Statement

Quantitative Real Time PCR analysis of *Sox9* and *Krt19* at 4 hours following acute pancreatic injury in Figure 3.3 was carried out by Claire Young. Trichrome staining in Figure 3.12 was completed by Nawab Azizi. All other experimental work presented was carried out by Jelena Toma.

Acknowledgments

First and foremost, I would like to thank my supervisor Dr. Chris Pin. The patience you have had over the last two years with someone who is inherently hard on themselves could not have been easy, but it has never gone unappreciated. Thank you for this amazing opportunity and for always being a supportive mentor.

To my parents and brother, Irena and Andrija Toma, and Luka Toma. Thank you for always having listening ears no matter the time of day. I will never be able to put into words how much I appreciate everything you have done for me. Thank you for never letting me doubt myself and forcing me to push through the tough times. Hvala – volim vas PUNO.

To Alen, thank you for being so kind and patient. Your easy-going attitude is the balance I sometimes need to be reminded of. Thank you for always knowing how to make me laugh. I love you so much!

To past and present members of the lab, this experience would not have been what it was without you. Charis, thank you for teaching me and for always willing to help me move my project forward. To Kurt, Ryan, Claire, and Melissa, thank you. I am so lucky that this experience has not just given me intelligent peers, but true and kind friends. I will miss our sarcastic jokes and the daily laughs.

I would also like to acknowledge my committee members, Dr. Donglin Bai and Dr. Cheryle Seguin for their guidance in completion of my project. Special thank you to Dr. Seguin for reviewing my thesis.

Finally, a thank you to all other friends and family members who have supported me in this adventure, and the adventures to come. It is always appreciated.

This experience has taught me to trust my instincts and always persevere. I will be forever grateful for this opportunity. On to the next chapter!

Table of Contents

List of Tables

List of Figures

List of Appendices

List of Abbreviations

ADM   Acinar-to-duct cell metaplasia

AGR2   Evidence of anterior gradient 2

AKT   Protein kinase B

ATF/CREB   Activating transcription factor/cAMP responsive element binding

ATF3   Activating Transcription Factor 3

ATF6   Activating Transcription Factor 6

bHLH   Basic helix-loop-helix

BSA   Bovine Serum Albumin Fraction V

bZIP   Basic leucine zipper

C/EBPα   CCAAT/enhancer-binding protein alpha

CARE   C/EBP-ATF response element

CCK   Cholecystokinin

CHOP   DNA damage inducible transcript 3

CIP   Cerulein Intraperitoneal

CP   Chronic Pancreatitis

CPA1   Carboxypeptidase A1

Ct   Cycle Threshold

CTCR   Chymotrypsinogen C

DAPI	4',6-diamidino-2-phenylindole
EGF	Epidermal growth factor
EGFR	Epidermal growth factor receptor
eIF2α	Eukaryotic initiation factor 2 alpha
ER	Endoplasmic Reticulum
ERAD	ER associated degradation
FITC	Fluorescein isothiocyanate
H&E	Hematoxylin & Eosin
H3k27ac	K27 acetylated histone H3
HDAC	histone deacetylase
Hnf6	Hepatocyte nuclear factor 6
I.P.	Intraperiotenal
IF	Immunofluorescence
IL	interleukin
IRE1	Inositol-requiring enzyme 1
JNK	Janus kinase
JUN	Transcription Factor AP-1
KEGG	Kyoto Encyclopedia of Genes
KRAS	Kirstan Ras
Krt19	Cytokeratin 19

mL	Millilitres
mM	Millimolar
Mrpl	Mitochondrial Ribosomal Protein
NFDM	Non-fat dried milk
NFκB	Nuclear factor kappa-light-chain-enhancer of activated B cells
ng	Nanograms
nM	Nanomolar
Nr5a2	Nuclear receptor subfamily 5 group A member 2
OVCA	Ovarian cancer
PBS	Phosphate Buffer Solution
PCR	Polymerase Chain Reaction
PDAC	Pancreatic Ductal Adenocarcinoma
Pdx1	Pancreatic and duodenal homebox 1
PERK	PKR-like Endoplasmic Reticulum Kinase
PI3k	Phosphoinositide 3-kinase
PRSS1	Cationic trypsinogen gene
PTEN	Phosphate and tensin homolog
Ptf1a	Pancreas specific transcription factor 1a
Rbpj	Recombining binding protein suppressor of hairless
SAL	Saline

SDS	Sodium dodecyl sulfate
Sox9	Sry-related high-mobility group box 9
SPINK1	Serine protease inhibitor Kazal type I
STAT3	Signal tranducer and activator of transcription 3
TBS	Tris Buffered Solution
TGFα	Transforming Growth Factor Alpha
TTR	Transthyrein
UPR	Unfolded Protein Response
Xbp	*X-box-binding protein*
μg	Micrograms
μl	Microlitres
μm	Micrometres

Chapter 1

1   Introduction

1.1   Overview

Pancreatitis is a debilitating disease defined by inflammation and fibrosis of the exocrine

pancreas (Roberts, 2015). Patients diagnosed with pancreatitis are 20 to 60 times more

likely to develop pancreatic ductal adenocarcinoma (PDAC), which has a 6-7% survival

rate 5 years post-diagnosis (Yadav & Lowenfels, 2013). The factors that link these

diseases together are not well understood. Genes involved in stabilization of the mature

acinar cell phenotype often have altered expression in pancreatic injury models (Jensen *et

al.*, 2005; Kowalik *et al.*, 2007). In contrast, mutations of developmental genes are rare in

PDAC patients, suggesting alternative mechanisms promote acinar cell de-differentiation

and cancer progression. Our lab has identified Activating Transcription Factor 3 (ATF3),

a transcription factor upregulated following activation of the unfolded protein response

(UPR), as a potential factor affecting acinar cell gene expression during pancreatitis

leading to acinar-to-duct cell metaplasia (ADM), a precursor phenotype of PDAC (Jensen

et al., 2005; Shi *et al.*, 2013). The goal of my research is to determine whether ATF3 is a

potential link between chronic pancreatitis (CP) and increased susceptibility to PDAC,

and to elucidate the signalling pathways by which ATF3 regulates ADM.

1.2   Pancreatitis

The pancreas develops from the endoderm and is divided into endocrine and exocrine portions (Jennings *et al.*, 2015). The exocrine pancreas represents 98% of the total volume and is composed of two specialized cell types: acinar cells and duct cells (Williams, 2010). Acinar cells are responsible for the release of digestive pro-enzyme containing zymogen granules, while duct cells release enzymes, ions and water into the gastrointestinal tract (Williams, 2010; Reichert & Rustgi, 2011). Dysregulation of exocytosis can lead to initiation of the inflammatory response, and loss of epithelial tissue. This pathological process is known as pancreatitis. Pancreatitis is a disease of the pancreas associated with auto-digestion leading to inflammation and fibrosis (Roberts, 2015; Storz, 2017). Pancreatic enzymes are pre-maturely activated in acinar cells leading to tissue destruction (Papachristou *et al.*, 2007). Acute episodes of pancreatic injury are reversible, and complete pancreatic regeneration occurs within 7 days in mouse models of pancreatitis (Grady *et al.*, 1998; Yadav *et al.*, 2011). However, chronic injury leads to extensive damage and fibrosis through alterations in cell organization, cytokine production and stellate cell activation (Grady *et al.*, 1998; Papachristou *et al.*, 2007; Aghdassi *et al.*, 2011). Most cases of pancreatitis are caused by excessive alcohol consumption, or gall stone obstruction from the bile duct (Roberts, 2015). In addition, there are cases of hereditary pancreatitis, in which certain genetic mutations promote disease progression (Aghdassi *et al.*, 2011; Roberts, 2015). These mutations are typically related to digestive enzyme activation, such as *PRSS1* (cationic trypsinogen gene), *SPINK1* (serine protease inhibitor Kazal type I), and *CTRC* (chymotrypsinogen C) (Whitcomb, 2010; Roberts, 2015).

Patients diagnosed with pancreatitis are more likely to develop PDAC (Lowenfels, 2006;

Yadav *et al.*, 2011), which is associated with extensive fibrosis, inflammatory infiltration,

and acinar cell atrophy (Logsdon & Ji, 2013). The factors that link these diseases together

are not well understood and therefore understanding the mechanisms of pancreatic injury

are crucial in developing preventative or therapeutic strategies to decrease the incidence

of PDAC.

1.2.1   Cell Responses to Injury

Following pancreatitis, the pancreas is challenged to regenerate and replenish damaged

cells (Murtaugh & Keefe, 2015). Injury stimulates a de-differentiation of acinar cells to a

progenitor-like phenotype, followed by proliferation, before re-differentiation into mature

acinar cells (Jensen *et al.*, 2005; Hess *et al.*, 2011). However, if this regenerative process

is compromised by recurrent injury, the ability of cells to re-differentiate to the acinar

phenotype is lost and this leads to an increased potential for oncogenic transformations.

This process is termed acinar-to-ductal metaplasia (ADM), and has been extensively cited

as a precursor phenotype to PDAC (Logsdon & Ji, 2009; Morris *et al.*, 2010; Shi *et al.*,

2013; Krah *et al.*, 2015). Histologically, ADM appears in both human and mouse tissue

as the accumulation of tubular complexes (**Figure 1.1**; Hess *et al.*, 2011; Prevot *et al.*,

2012). While there is still debate regarding the true cellular basis of pancreatic

metaplasia, it is widely accepted that ADMs are derived, at least in part, from an existing

acinar population that has undergone de-differentiation (Means *et al.*, 2005; Houbracken

et al., 2016). ADM is an early event in PDAC development and is thought to be the

source of neoplasias
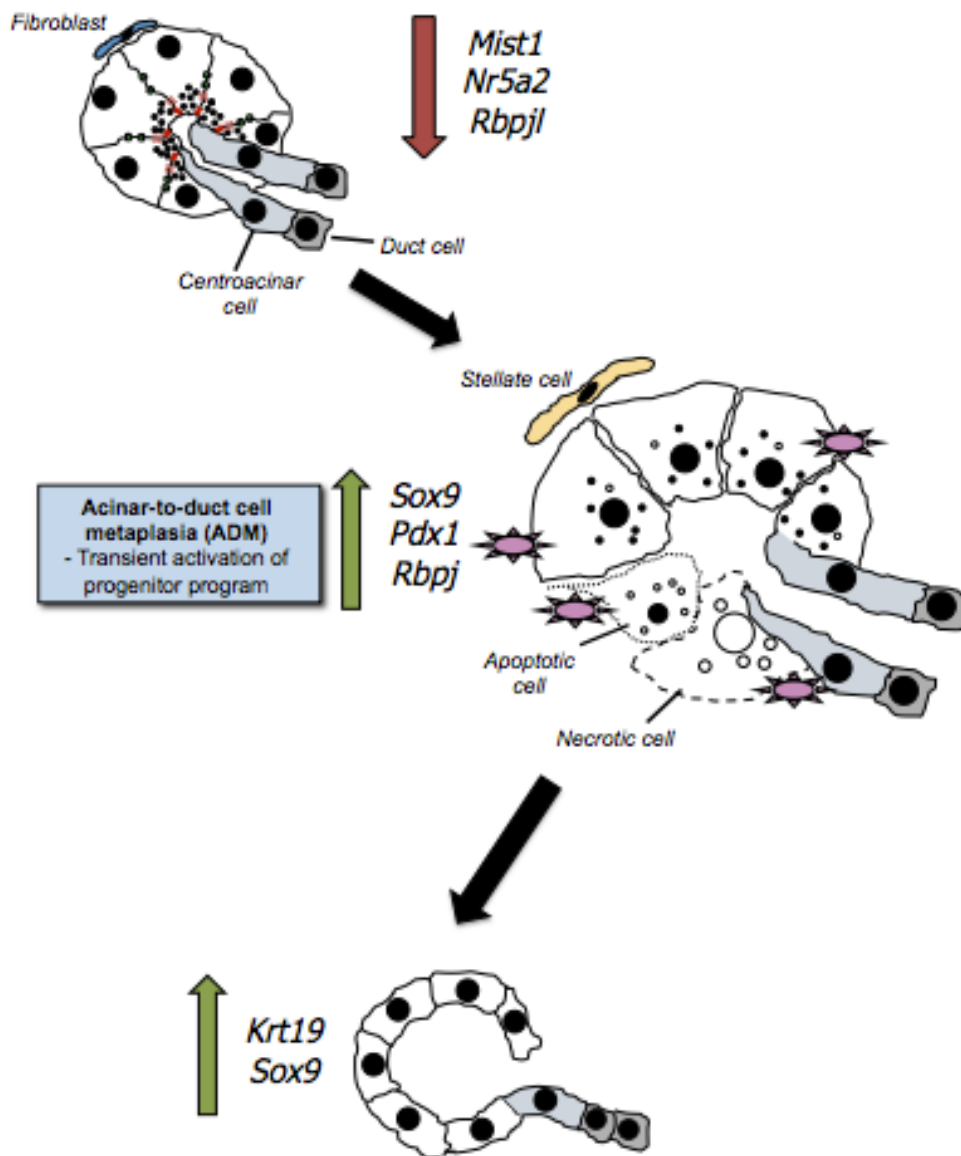
Figure 1.1 Schematic illustration depicting acinar-to-duct cell metaplasia

Following pancreatitis, acinar cells are stimulated to de-differentiate in an attempt to repopulate damaged areas. If this process is compromised, acinar cells can de-differentiate into a progenitor-like cell, then re-differentiate into a duct-like cell in a process term acinar-to-duct cell metaplasia (ADM). This process is driven by decreases in the acinar transcriptional program (*Mist1, Nr5a2, Rbpjl*), and increases in progenitor and ductal programs (*Sox9, Pdx1, Rbpj, Krt19*).

(Scotti *et al.*, 2012). These cells transform into pre-malignant cells, and can become cancerous when persistent growth factor signalling is present (Ebine *et al.*, 2016). Development of the ADM phenotype occurs through a fine-tuned transcriptional program in which there is a loss of the mature acinar program, and an upregulation of the progenitor and ductal program (Rooman & Real, 2012; Ebine *et al.*, 2016). Identifying the molecular factors responsible for this transformation is crucial to understand the initiation of the ADM process, and how this increases susceptibility to PDAC development (**Figure 1.1**).

1.2.2 Cellular and Molecular Events in ADM

Several transcription factors are responsible for regulating the acinar differentiation program. When these factors become differentially expressed, either through experimental knockout models, or downregulation in human disease, loss of acinar identity occurs thereby allowing ADM (Prevot *et al.*, 2012; von Figura *et al.*, 2014; Storz, 2017). Normal acinar and duct development occurs through a differentiation process whereby endoderm cells differentiate to pancreatic progenitor cells through combined expression of pancreatic and duodenal homeobox 1 (PDX1), pancreas transcription factor 1a (PTF1A), recombining binding protein suppressor of hairless (RBPJ) and Sry-related high-mobility group box 9 (SOX9) (von Figura *et al.*, 2014; Jennings *et al.*, 2015; Storz, 2017). Acinar cells require the expression of PTF1A/RBPJL, nuclear receptor subfamily 5 group A member 2 (NR5A2*)*, MIST1 and GATA6 for complete differentiation, whereby ductal cells differentiate through factors such as hepatocyte nuclear factor 6 (HNF6), and SOX9 (Pin *et al.*, 2000; von Figura *et al.*, 2014; Jennings *et al.*, 2015). Re-

establishing a progenitor-like transcriptional profile is part of the process of ADM (**Figure 1.1**, Means *et al.*, 2005).

A key regulator for the maintenance of acinar cell identity is MIST1, a basic helix-loop-helix (bHLH) transcription factor responsible for regulating acinar cell maturation and function (Pin *et al.*, 2000; Shi, 2009). Germ line deletion of *Mist1* leads to incomplete acinar cell maturation and pre-mature enzyme activation (Pin *et al.*, 2001; Johnson *et al.*, 2004). This increases sensitivity to pancreatitis due to changes in intracellular communications and exocytosis (Kowalik *et al.*, 2007; Shi, 2009). In addition, *Mist1* deletion in combination with expression of cancer promoting factors (such as activated Kirstan Ras (KRAS)) accelerates ADM and PDAC development, while forced *Mist1* expression prevents KRAS-induced neoplasia formation (Shi, 2009; Johnson *et al.*, 2012).

RBPJ and RBPJL, contribute to a progenitor or mature acinar cell phenotype, respectively, through interaction with the PTF1A complex. In pancreatic progenitor cells, RBPJ is part of the PTF1A complex targeting PTF1A to genes involved in cell cycle regulation. As cells mature to an acinar cell fate, the PTF1A complex binds to the *Rbpjl* promoter to increase transcription. RBPJL replaces RBPJ in the PTF1A complex and binds gene promoters necessary for acinar cell development (Masui *et al.*, 2010; Krah *et al.*, 2015). If *Ptf1a* is lost in murine (6-8 weeks old) acinar cells, they become sensitized to KRAS-oncogenic transformation. This prompts rapid and extensive ADM (Krah *et al.,* 2015).

NR5A2 is another factor that co-operates with the PTF1 complex to regulate acinar function through maintenance of genes involved in exocytosis. NR5A2 is of particular interest in an injury model as it is critical for regeneration following acute pancreatitis (von Figura *et al.*, 2014). While not necessary for pancreatic development, loss of *Nr5a2* leads to a downregulation of factors indicative of terminally differentiated acinar cells (i.e. *Mist1* and Carboxypeptidase A1 (*CPA1*)), and ultimately increases the capacity of acinar cells to undergo ADM (von Figura *et al.*, 2014). This creates a permissive environment to drive neoplasia and cancer. In contrast, GATA6 is required for complete maturation and maintenance of acinar differentiation by regulating gene expression of maturation factors such as *Mist1* and *Rbpjl* (Martinelli *et al.*, 2016). Loss of GATA6 results in acinar atrophy, incomplete acinar differentiation, and promotes persistent ADM (Martinelli *et al.*, 2016; Storz, 2017). Evidence of GATA6 loss in human PDAC suggests that it acts as a tumour suppressor, since increased expression locks epithelial cells in a differentiated state, and blocks cancer formation (Martinelli *et al.*, 2016).

Expression of progenitor and ductal markers are essential in driving the metaplastic phenotype (Means *et al.*, 2005; Ebine *et al.*, 2016; Storz, 2017). In normal acinar cells, *Sox9* is expressed in low levels (Jensen *et al.*, 2005; Storz, 2017). Ductal factors are expressed in pancreatic acinar cells prior to transformation, thereby priming cells for ADM. HNF6 is responsible for inducing *Sox9* expression, which remains elevated in ADM (Prevot *et al.*, 2012). SOX9 also induces expression of *Krt19*, a duct-specific marker (Kopp *et al.*, 2012). SOX9 is required for neoplastic formation, as loss of *Sox9* in combination with additional PDAC promoting factors did not affect pancreas morphology (Kopp *et al.*, 2012). In addition to *Sox9*, *Pdx1* is upregulated during

pancreatitis and PDAC, and is believed to aid in driving the process of ADM (Miyatsuka, 2006; Storz, 2017). *Pdx1* is expressed in pancreatic progenitor cells, which give rise to specialized cells of both endocrine and exocrine tissue. *Pdx1* is typically downregulated after late embryonic development, but is increased in patients and mouse models of PDAC (Miyatsuka, 2006). PDX1 regulates ADM through signal transducer and activator of transcription 3 (STAT3), a regulator of stem cell self-renewal and inflammation (Miyatsuka, 2006).

These changes in gene expression that occur are a result of acinar cell plasticity (Stanger & Hebrok, 2013). When exposed to injury, acinar cells readily de-differentiate to repopulate damaged areas (Jensen *et al.*, 2005). In addition to these genetic changes that drive the ADM process, additional signalling pathways are upregulated that are known to initiate and maintain the de-differentiation and trans-differentiation processes.

1.3   Signalling Pathways in Acinar-to-Duct Metaplasia

Pancreatitis leads to activation of signalling pathways that are required to initiate and maintain the de-differentiation and trans-differentiation processes. *In vitro* evidence suggests that multiple factors are implicated in driving the ADM process, including increased epidermal growth factor receptor (EGFR) signalling (Means *et al.*, 2005; Ardito *et al.*, 2012; Eser *et al.*, 2014). ADM was demonstrated in 3D acinar cultures following EGFR pathway activation (Means *et al.*, 2005; Scotti *et al.*, 2012). Therefore, understanding EGFR signalling, and its effects in cancer development, is necessary to determine increased susceptibility to PDAC following chronic pancreatitis.

EGFR has been implicated in the pathogenesis of many epithelial cancers through inappropriate activation caused by mutations or increased expression of ligands. EGFR is a cell surface receptor belonging to the ErbB family of tyrosine kinases (Ardito *et al.*, 2012; Yewale *et al.*, 2013). EGFR consists of an extracellular signalling domain, a hydrophobic transmembrane domain, an intracellular catalytic tyrosine kinase domain, and several cytosolic tyrosine residues. When ligands, such as epidermal growth factor (EGF) or Transforming Growth Factor Alpha (TGFα) bind to the EGFR extracellular domain, receptor dimerization and activation occurs through auto-phosphorylation (Yewale *et al.*, 2013). These phosphorylated regions act as docking sites for cytosolic proteins responsible for activating downstream events such as proliferation, survival, and cell differentiation (Yewale *et al.*, 2013; Logsdon & Lu, 2016). The activation of EGFR leads to induction of several downstream signalling pathways including phosphoinositide 3-kinase (PI3K), phosphate and tensin homolog (PTEN), protein kinase B (AKT), RAS, and janus kinase (JAK)/STAT (Fitzgerald *et al.*, 2015; Logsdon & Lu, 2016). Of particular interest to ADM development is the RAS pathway, as mutations in the RAS protein, specifically *KRAS*, have been implicated in PDAC development (Logsdon & Ji, 2009). The RAS pathway consists of the following proteins: Raf (MAPKKK), MEK1/2 (MAPKK) and ERK1/2 (MAPK) (Fitzgerald *et al.*, 2015). Raf kinase phosphorylates and activates MEK1/2, which in turn can phosphorylate and activate ERK1/2. Active ERK proteins activate a variety of downstream cytosolic and nuclear proteins, including nuclear factor kappa-light-chain-enhancer of activated B cells (NFκB) or Transcription Factor AP-1 (JUN), that are responsible for regulating gene expression (**Figure 1.2**; Chang *et al.*, 2003; Molina & Adjei, 2006; Roberts & Der, 2007).
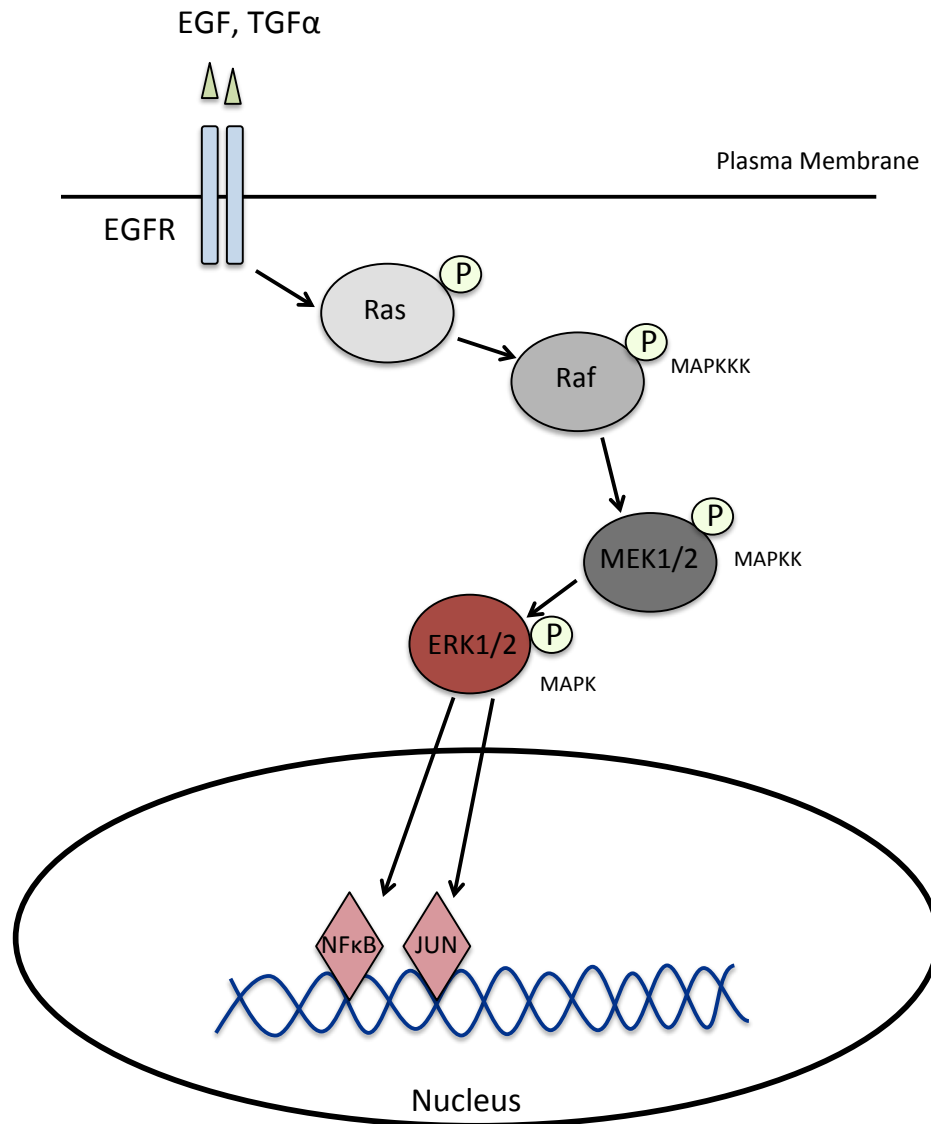
Figure 1.2 Schematic depiction of the Epidermal Growth Factor Receptor Signalling Pathway

The Epidermal Growth Factor Receptor (EGFR) Signalling Pathway is responsible for regulating cellular processes, such as proliferation and cell cycle progression. Ras phosphorylates and activates Raf, which sequentially activates Mek1/2, and then ERK1/2. ERK proteins activate cytosolic and nuclear proteins, such as nuclear factor kappa-light-chain-enhancer of activated B cells (NFκB) or Transcription Factor AP-1 (JUN), responsible for regulating gene expression.

Dysregulation of the EGFR pathway is common; over 90% of pancreatic cancer cases present with a constitutively active mutation in the KRAS protein (Molina & Adjei, 2006; Aghdassi *et al.*, 2011; Guerra & Barbacid, 2013; Logsdon & Lu, 2016). The most common KRAS mutation, a single nucleotide substitution termed KRAS[G12D], leads to constitutive signalling and increased proliferation and cell survival, promoting a cancerous phenotype. Evidence of EGFR signalling in ADM and pancreatic cancer development has become a widely studied topic (Molina & Adjei, 2006; Storz, 2017).

Following exposure of pancreatic injury, acinar cells increase EGFR signalling (Ardito *et al.*, 2012). Activation of EGFR signalling in murine pancreata induces ADM and formation of PDAC (Means *et al.*, 2005; Scotti *et al.*, 2012). This is a cell autonomous event as treatment of isolated primary pancreatic acinar cells with TGFα induces transformation into metaplastic duct structures (Means *et al.*, 2005; Liou *et al.*, 2015). EGFR is necessary for ADM since inhibition with the EGFR inhibitor erlotinib leads to normal, non-transformed tissues that present with less duct-like cells. Complete ablation of *Egfr* eliminates TGFα induced metaplasia *in vivo*. All components of the EGFR pathway are necessary to transduce signals, as inhibition of downstream factors, such as MEK, also lead to decreased trans-differentiation (Ardito *et al.*, 2012).

Evidence of increased EGFR signalling is also present in cases of human pancreatic cancer (Molina & Adjei, 2006; Guerra & Barbacid, 2013; Shi *et al.*, 2013). In addition to an increased accumulation of EGFR and its ligands in patients with chronic pancreatitis and PDAC, there is evidence of KRAS mutations (Molina & Adjei, 2006; Roberts & Der, 2007; Morris *et al.*, 2010). While direct inhibition of EGFR has not proven to be a

successful therapeutic, in combination with additional therapies and signalling blockades it may be a promising avenue to explore.

Mutant forms of KRAS on their own do not cause the development of ADM and PDAC (Morris *et al.*, 2010; Eser *et al.*, 2014; Logsdon & Lu, 2016). Secondary events are necessary to push the phenotype, including loss of terminal acinar differentiation factors (such as *Mist1* or *Nr5a2*), or initiation of inflammatory pathways (Shi, 2009; Masui *et al.*, 2010; Logsdon & Lu, 2016; Storz, 2017). To fully understand the mechanism by which ADM develops, it is important to investigate additional pathways that become affected during pancreatitis.

1.4   The Unfolded Protein Response

1.4.1   General Overview

The unfolded protein response (UPR) is a cell stress response mechanism that is activated by Endoplasmic Reticulum (ER) stress (Harding *et al.*, 2000; Kubisch *et al.*, 2006; Thompson *et al.*, 2009). The UPR is a highly conserved pathway between yeast and mammals and serves an important function in maintaining protein homeostasis in the cell (Lee *et al.*, 2002; Iwawaki *et al.*, 2010). ER stress occurs when protein folding demand exceeds folding capacity. Such demands can be placed on the cell through changes to gene expression, gene mutations, or environmental factors such as nutrient starvation, ischemia, viruses, or changes in temperature (Lee, 1992; Bernales, 2006; Wu & Kaufman, 2006; Maas & Diehl, 2015). These changes can be detrimental to normal cell function, so the cell must find ways to accommodate these changes to persist survival. To

do so, the cell activates the UPR, which involves signaling between the ER and the nucleus (Bernales, 2006; Wu & Kaufman, 2006; Thompson *et al.*, 2009).

Under physiological conditions, plasma membrane proteins travel to the ER where proper folding is facilitated by ER-resident chaperones. If the ER senses an increased demand for folding capacity, the UPR is activated leading to enlargement of the ER, and increased expression of chaperone proteins (Harding *et al.*, 2000; Kubisch *et al.*, 2006; Sah *et al.*, 2014). However, if the cell is stressed beyond the point of capacity, the UPR activates pathways to decrease protein translation, decrease overall loading of proteins onto the ER, or target unfolded/misfolded proteins for degradation, via ER associated degradation (ERAD) (Wu & Kaufman, 2006; Wu *et al.*, 2007; Maas & Diehl, 2015). If the UPR is activated for a prolonged period, and none of these mechanisms compensate for the changes in protein levels to restore homeostasis, the cell will be targeted for apoptosis to prevent accumulation of damaged proteins (Lee *et al.*, 2002; Bernales, 2006). The coping mechanisms outlined above are activated through three specific arms of the UPR pathway: PKR-like Endoplasmic Reticulum Kinase (PERK), Inositol-requiring enzyme 1 (IRE1), and Activating Transcription Factor 6 (ATF6) (Lee, 1992; Haze *et al.,* 1999; Harding *et al.*, 2000; Bernales, 2006; Liang *et al.*, 2006).

PERK, IRE1, and later ATF6, are activated in response to ER stress through dissociation from BiP/GRP78, an ER resident chaperone protein part of the Hsp70 family (Wei *et al.*, 1995; Bernales, 2006). The first immediate response is PERK and IRE1. Each pathway is activated by dimerization, and autophosphorylation (Harding *et al.*, 2000; Ron *et al.*, 2000). PERK pathway activation leads to eukaryotic initiation factor 2 alpha (eIF2α) phosphorylation, decreased protein translation in the cell, and increased translation of

downstream proteins (ATF4) that function as transcription factors (Haze *et al.*, 1999;

Bernales, 2006; Zhang *et al.*, 2008). IRE1 activates endoribonuclease activity, leading to

altered splicing of *X-box-binding protein* (*Xbp*) *1* mRNA, allowing it to generate a

transcription factor (spliced [s] XBP1), which increases expression of ER-chaperone

proteins and activates ERAD (Calfon *et al.*, 2002; Lee *et al.*, 2002; Wu & Kaufman,

2006; Sah *et al.*, 2014). ATF6 becomes activated through translocation to the cis-golgi

compartment, where it is cleaved by site-1 and -2 proteases. Cleaved ATF6 is then

translocated to the nucleus to increase transcription of ER-chaperone proteins, and elicit

transcriptional activity alongside ATF4 and sXBP1 (Haze *et al.*, 1999; Bernales, 2006;

Wu & Kaufman, 2006). These pathways function to maintain physiological levels of

protein in the cell (**Figure 1.3**). This is especially important in pancreatic acinar cells, as

they are subjected to high levels of stress, due to the higher than average protein demand

(Kubisch *et al.*, 2006; Iwawaki *et al.*, 2010). While the primary function of the UPR is to

maintain homeostatic levels of protein, it can contribute to development of pathological

processes as well, including pancreatitis (Kubisch *et al.*, 2006; Lugea, 2011; Sah *et al.*,

2014; Karki *et al.*, 2015).

1.4.2 Involvement of UPR in Pancreatitis and PDAC

Due to the acinar cells' large demand for protein synthesis and activity, they are

subjected to higher than normal stress levels (Kubisch *et al.*, 2006). Acute or chronic

exposures to elevated stress signals leads to disruption in protein homeostasis in the cell,

and initiation of pancreatitis. The ER stress response becomes activated in stressed
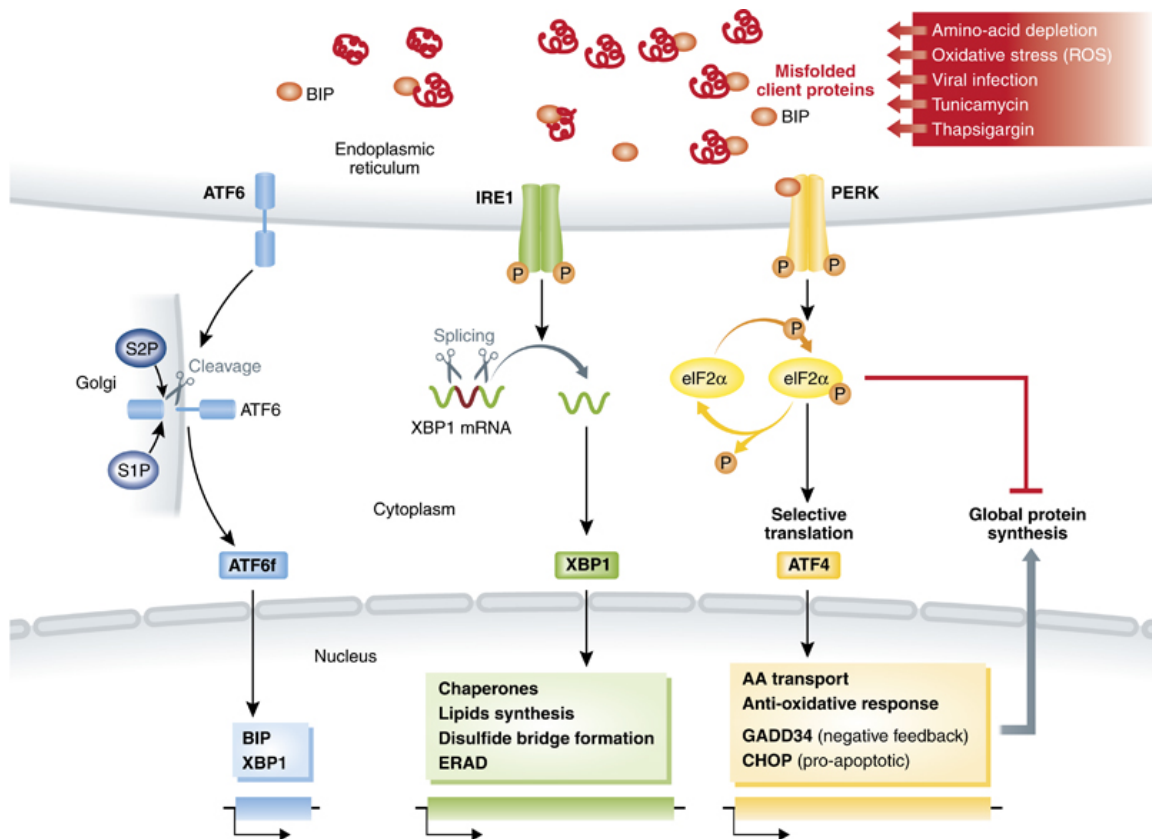
Figure 1.3 The Unfolded Protein Response

The unfolded protein response (UPR) is a cell stress mechanism responsible for maintaining protein homeostasis. The Endoplasmic Reticulum (ER) senses when the protein folding demand of the cell exceeds its capacity. The ER will activate 3 specific signalling pathways, PKR-like Endoplasmic Reticulum Kinase (PERK), Inositol-requiring enzyme 1 (IRE1), and Activating Transcription Factor 6 (ATF6), in an attempt to decrease protein translation, decrease protein load, target proteins for degradation, and finally if stress is unresolved, activate cellular apoptosis. All 3 pathways are responsible for activating proteins that will act as transcription factors to aid in activation and regulation of these processes (Cláudio *et al.*, 2013).

pancreatic acinar cells, as evidenced by increased expression of genes that are targets of ER stress mechanisms (Sah *et al.*, 2014). Pancreatic acinar cells increase the ER stress response in response to multiple environmental stimuli used in mouse models of pancreatitis, including forced cholecystokinin (CCK) receptor activation through cerulein injections, injections of L-arginine, and through ethanol feeding (Liang *et al.*, 1996; Kubisch *et al.*, 2006; Kowalik *et al.*, 2007; Lugea, 2011).

Regardless of the method by which pancreatitis is initiated, the UPR is rapidly activated. Following induction of pancreatitis by cerulein injections, PERK and IRE1 are activated by autophosphorylation (Liang *et al.*, 2006). A similar effect is observed when mice are administered L-arginine, as activation of all major UPR pathways were detected within 4 hours of pancreatitis initiation (Lugea, 2011). While chronic alcohol consumption may be a predisposing factor to pancreatitis development in murine models and humans, exposure to this insult alone does not cause the disease to progress. However, ethanol exposure leads to increased UPR activity, as evidenced by increased spliced XBP1 levels (Lugea, 2011; Alahari *et al.*, 2011). This may underlie the susceptibility to pancreatitis if the acinar cells are exposed to additional injury. In addition to UPR activation in the L-arginine and cerulein treated models, there is evidence of upregulation of downstream transcription factors that regulate the UPR response, such as ATF4, ATF3, and CCAAT/enhancer-binding protein alpha (C/EBPα) (Ji *et al.*, 2003; Kubisch *et al.*, 2006).

The primary function of the UPR is to maintain protein homeostasis (Bernales, 2006). However, in instances where the cell has an overwhelming amount of damaged protein, prolonging survival of the cell may be detrimental. In this case, the UPR now becomes pathological. This is especially true of cancerous cells (Gifford *et al.*, 2016). Cancer cells

are constantly under ER stress due to hypoxic conditions, low nutrients, and high loads of mutant protein (Namba & Kodama, 2015). There is evidence in pancreatic cancer that the UPR promotes chemo-resistance through BiP/GRP78 expression. GRP78, an ER-chaperone protein, activates anti-apoptotic pathways leading to chemo-resistant tumours. This demonstrates how UPR activation, and in turn BiP/GRP78 expression, can no longer function to maintain physiological protein levels, but actually promote a cancerous phenotype (Gifford *et al.*, 2016).

Defining the function of downstream transcription factors of the UPR will help in understanding the role of the UPR in pancreatitis and PDAC development. Since these factors do not have roles exclusive to protein homeostasis but may also contribute to the promotion of pancreatic disease, studying them may identify mechanisms of pancreatic disease development.

1.5 Activating Transcription Factor 3

1.5.1 General Overview

The activating transcription factor/cAMP responsive element binding (ATF/CREB) proteins belong to the basic leucine zipper (bZIP) family of transcription factors. All ATF/CREB proteins bind to similar consensus sites and can be grouped based on their amino acid similarities (Hai & Hartman, 2001). These subgroups include ATF1, 2, 3, 4, 6, and 7, which share the bZIP binding element (Hai & Hartman, 2001; Thompson *et al.*, 2009). BZIP proteins can bind to DNA as homodimers with each other, or heterodimers with other transcription factors including C/EBP, AP1, p53, and SMAD (Thompson *et*

al., 2009; Wang *et al.*, 2015). Depending on the binding partner, this can affect the DNA binding specificity and transcriptional activities (Hai & Hartman, 2001).

ATF3 is 181 amino acids, has a molecular mass of 22 kDa, and has only one defined functional domain - the bZIP domain (Thompson *et al.*, 2009). ATF3 interacts with other ATF/CREB proteins, and depending on the promoter it is bound to, can act as an activator or repressor of transcription (Hai & Hartman, 2001; Thompson *et al.*, 2009). The *Atf3* promoter contains ATF/CRE and AP1 sites indicating it is regulated by other ATF proteins. *Atf3* is a stress-inducible gene. *Atf3* mRNA expression is low in quiescent cells, but is induced by a variety of stress signals (Hai & Hartman, 2001; Lu *et al.*, 2006; Thompson *et al.*, 2009). ATF3 expression is increased in a variety of tissues, including heart, liver, kidney, and skin, in response to ischemia, hypoxia, direct mechanical or chemical injury, or wounding (Hai & Hartman, 2001; Pelzer *et al.*, 2006; Lu *et al.*, 2006; Li *et al.*, 2010). Cellular stress signals, such as elevated temperature, cytokine, genotoxic agents, cytotoxic agents, ER stress and DNA damage, also increase ATF3 expression *in vitro* (Li *et al.*, 2010; Wang *et al.*, 2015; Zhao *et al.*, 2016).

Atf3 mRNA expression is increased within 2 hours of stress stimulation in mouse embryonic fibroblast cells, in this case by thapsigargin treatment and amino acid starvation (Liang *et al.*, 1996; Jiang *et al.*, 2004). This quick response indicates its direct activation by cellular stress response mechanisms, such as the UPR (Liang *et al.*, 1996; Bernales, 2006). Studies have shown that activation of the UPR leads to phosphorylation and increased expression of ATF2 and cJUN, through activation of the IRE1 pathway (Jiang *et al.*, 2004), which can target and regulate promoters containing ATF/CRE or AP1 sites (Liang *et al.*, 1996). cJUN and ATF2 have been shown to work in co-operation

to bind to the *Atf3* promoter and activate its transcription (Liang *et al*., 1996; Jiang *et al*., 2004). In addition, other arms of the UPR pathway, such as PERK or ATF6, have also been shown to increase *Atf3* expression (Jiang *et al*., 2004; Kowalik *et al*., 2007). The PERK pathway, upon stress induction, leads to phosphorylation of eIF2α, which blocks its ability to associate in a transcriptional complex, and decreases protein translation and increases ATF4 expression. ATF4 goes on to then increase *Atf3* expression through binding to a C/EBP-ATF response element (CARE) located on the *Atf3* promoter (**Figure 1.4**) (Bernales, 2006; Kowalik *et al.*, 2007; Fu & Kilberg, 2013). *Atf3* expression is then maintained through blocking of the negative feedback mechanism on eIF2α (Kowalik *et al*., 2007). The activation of ATF3 is dependent on this pathway as deletion of eIF2 kinase blocks synthesis of *Atf3* mRNA and protein (Jiang *et al*., 2004). As well, in conjunction with eIF2α, ATF6 increases expression of *Atf3* (Kubisch *et al*., 2006).

Atf3 expression is increased through cellular stress mechanisms both directly and indirectly (Hartman *et al.*, 2004; Li *et al.*, 2010; Kwon *et al.*, 2015). The increase in expression following stress exposure suggests the roles ATF3 may play following UPR activation. Understanding how ATF3 may be eliciting its effects as a transcription factor will provide insight into how it may regulate outcomes in damaged acinar cells.
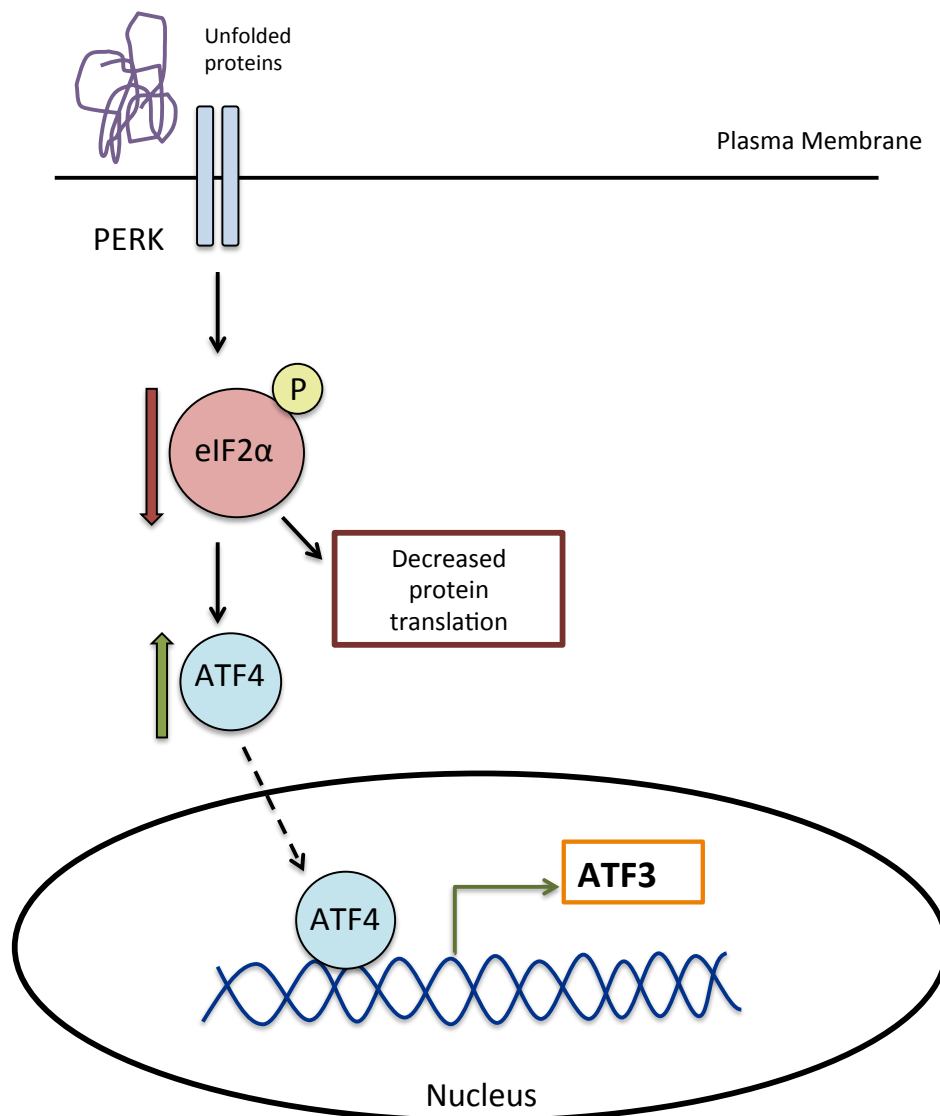
Figure 1.4 Schematic illustration of the pathways responsible for UPR-mediated induction of ATF3 expression

Activating Transcription Factor 3 (ATF3) is activated by the UPR through a variety of cellular stresses. Specifically, PERK proteins sense unfolded proteins in the extracellular space and phosphorylates and de-activates eiF2α, leading to decreased protein translation and increased ATF4 expression. ATF4 then translocates to the nucleus where it binds to C/EBP-ATF response element (CARE) sequences in the ATF3 promoter, activating its expression.

1.5.2   ATF3 Transcriptional Activity

There is some evidence that when ATF3 binds as a homodimer, it acts a transcriptional

repressor, and when bound as a heterodimer, it activates transcription (Zhao *et al.*, 2016).

ATF3 also exists in an alternatively spliced form that lacks the leucine zipper. The two

splice forms of the protein have different transcriptional functions. It has been suggested

that the full length isoform (181 amino acids) may repress rather than activate

transcription (Hashimoto *et al.*, 2002; Thompson *et al.*, 2009; Wang & Yan, 2015; Kwon

et al., 2015). The truncated ATF3 protein, termed ATFΔZip (135 amino acids), lacks the

leucine zipper domain, and can therefore not bind to DNA. This shorter isoform can

however bind to other transcription factors, and thereby inhibit binding to promoter

regions leading to inhibition of transcription (Hashimoto *et al.*, 2002; James *et al.*, 2006;

Wang & Yan, 2015; Kwon *et al.*, 2015).

More recently it has been recognized that the function of ATF3 depends on the

transcriptional complex it is a part of and the promoter region it is bound to, therefore the

role of ATF3 as a repressor or activator cannot be generalized (Thompson *et al*., 2009,

Zhao *et al*., 2016). ATF3 activates transcription through direct protein-protein

interactions with DNA damage inducible transcript 3 (CHOP), which leads to apoptosis

(Liang *et al*., 1996). ATF3 may also regulate gene expression through direct promoter

interactions, as evidenced by reduced inflammatory activation in injured kidney cells

when ATF3 recruits inhibitory histone deacetylase (HDAC) 1 to the NFκB promoter (Li

et al., 2010). ATF3 not only binds to promoter regions to elicit its effects, but also

interacts with enhancer regions, as defined by binding to p300 and K27 acetylated histone

H3 (H3k27ac) sites (Zhao *et al.*, 2016). In fact, ATF3 may act as a "primer" for other activating or repressing transcription factors, serving to recruit these proteins to enhancer regions to affect the transcriptional program (Zhao *et al.*, 2016). Overall, ATF3 plays a complex role in regulating transcriptional programs, and the protein interactions and genomic sites where ATF3 binds will define how and which transcriptional programs are being regulated (Li *et al.*, 2010; Zhao *et al.*, 2016)

1.5.3   Physiological protective roles of ATF3

ATF3 has been shown to have protective roles in certain physiological processes including inflammation and apoptosis. Specifically, ATF3 has been shown to negatively regulate transcription of pro-inflammatory cytokines and function as a tumour suppressor (Huang *et al.*, 2008; Li *et al.*, 2010; Kwon *et al.*, 2015).

Deletion of *Atf3* in primary macrophages leads to elevated expression of interleukin (IL)-6 and IL-12p40 pro-cytokines. This is specific to asthma, an inflammatory disease of the lungs, where *Atf3* null mice exhibit increased airway resistance corresponding to increased inflammatory cell infiltration (Gilchrist *et al.*, 2008; Thompson *et al.*, 2009). In addition to the roles in lung tissue, ATF3 has been shown to protect against acute kidney injury through regulation of NFκB in both a direct and indirect manner. Directly, ATF3 inhibits the inflammatory response following acute kidney damage by binding to the p65 subunit of NFkB, preventing nuclear translocation and downstream activation of inflammation (Kwon *et al.*, 2015). Indirectly, ATF3 recruits inhibitory HDAC1 to the NFkB promoter, therefore inhibiting expression of pro-inflammatory factors (Li *et al.*, 2010).

In addition to these anti-inflammatory effects, ATF3 can act in prostate cancer cells to induce apoptosis. KLF6, a tumour suppressor gene, acts directly on the *Atf3* promoter to increase expression, leading to apoptosis. The role of ATF3 as a tumour suppressor is supported by gene knockdown experiments, where loss of *Atf3* blocks apoptosis in prostate cancer cell lines (Thompson *et al.*, 2009; Wang *et al.*, 2015; Ebine *et al.*, 2016). Similarly, ATF3 functions in breast cancer cells to induce apoptosis and decrease metastatic potential. There is evidence that high progesterone levels, present in ovarian cancer (OVCA) cell lines, upregulates expression of *Atf3* and apoptosis. As well, ATF3 has been implicated in regulating the metastatic potential of OVCA cells as ectopic overexpression of ATF3 decreases invasiveness compared to controls (Syed *et al.*, 2005; Thompson *et al.*, 2009). Overall, these studies suggest the role of *Atf3* in decreasing the oncogenic potential in prostate and breast cancer cells through its ability to increase apoptosis and decrease invasiveness.

While ATF3 has been shown to have a protective role in certain physiological processes, such as inflammation or tumour suppression, there is evidence to suggest that it may have detrimental roles as well, and function to promote and maintain a pathological outcome (Bandyopadhyay *et al.*, 2006; Pelzer *et al.*, 2006; Thompson *et al.*, 2009).

1.5.4   ATF3 in pathology

Expression of ATF3 is induced by elevated stress through direct disruption of normal cell function, such as DNA damage, or through cancer promoting environmental signals, such as ultraviolet radiation (Pelzer *et al*., 2006; Zhao *et al*., 2016). Since ATF3's expression is associated with pathological factors, it is predictive that ATF3 would then be

associated with promoting oncogenic transformation of cells. This occurs in many tissues such as breast cancer, prostate cancers and lymphomas (Thompson *et al.*, 2009). Although ATF3 can inhibit cell cycle progression in cancer cells, thereby decreasing cancer growth, there is evidence that overexpression of ATF3 in human prostate cancer cell lines led to increased proliferation and G1 to S growth phase transition (Pelzer *et al.*, 2006), while also promoting metastasis and increased invasiveness (Bandyopadhyay *et al.*, 2006). A similar effect is evident in Hodgkin lymphoma cells, where *Atf3* expression is increased through activation of c-JUN, and leads to increased proliferation and viability of these cells (Janz *et al.*, 2006). ATF3's regulation of these pro-cancer processes may be through inhibition of GADD153. Binding of ATF3 to the GADD153 promoter of HeLA cells induces cell cycle arrest and apoptosis provides mechanism to its oncogenic properties (Hartman *et al.*, 2004; Jiang *et al.*, 2016).

In addition to the role of ATF3 in cancer development, ATF3 can affects cell differentiation. While there is evidence for the role of ATF3 in promoting terminal differentiation (James *et al.*, 2006), it has also been implicated in cell de-differentiation. ATF3 represses adipocyte differentiation through direct transcriptional regulation. C/EBPα and PPARγ are transcription factors that play a critical role in the expression of adipose differentiation genes. Overexpression of ATF3 in 3T3-L1 cells, a cell line derived from fibroblasts, represses adipocyte differentiation through binding to ATF/CRE sites on the C/EBPα promoter (Jang *et al.*, 2012).

The presence of ATF3 in a variety of pathological tissues indicates the detrimental role it may play. Based on the literature, it is clear that the function of ATF3 can vary greatly depending on the tissue type and cell conditions. To understand the role that *Atf3* plays in

pancreatitis and ADM development, it is first necessary to explore its mechanism of action in other pancreatic processes.

1.5.5   ATF3 in the pancreas

In addition to the prominent roles ATF3 plays in apoptosis, cellular function and differentiation in other tissue types, there is evidence that ATF3 affects several processes in the pancreas. In pancreatic β-cells, ATF3 has been implicated in apoptosis, differentiation and increasing cell dysfunction (Piper *et al.*, 2004; Hartman *et al.*, 2004; Jang, 2011).

β-cell death is a significant factor in the etiology of type 1 and type 2 diabetes. Patients with these diseases show increased levels of *Atf3* in their islets. Cell death is promoted in this tissue through increased activation of NFκB and JNK signalling, both of which are responsible for activating *Atf3* expression. *Atf3* has been implicated in β-cell apoptosis, as islets deficient in ATF3 are protected from cytokine- and nitric oxide-induced apoptosis. The mechanism by which this occurs is speculated to be through direct interactions with Gadd34/CHOP. The formation of this complex leads to increased expression of specific pro-apoptotic genes. In this instance, the role of *Atf3* in the pancreas is detrimental to its function (Hartman *et al.*, 2004).

Atf3 has also been shown to play a pathological role in β-cell function. A study by Jang *et al.* in 2011 explores the role of ATF3 in regulating PDX1, a key factor of pancreatic development, β-cell differentiation, regeneration and maintenance of function. Activation of the ER stress pathway in β-cells affects PDX1 transcriptional activity. Since *Atf3* expression is upregulated during cell stress, its role in regulating *Pdx1* expression are

clear. Over-expression of ATF3 decreases *Pdx1* expression in β-cells through direct interactions with the *Pdx1* promoter, as mutations of the ATF3 binding site in the *Pdx1* promoter disrupted this repressive activity. Repression of *Pdx1* by ATF3 leads to suppression of insulin expression and secretion, decreasing β-cell functionality (Jang, 2011).

In addition to the role ATF3 plays in repressing β-cell functionality, it may also affect β-cell differentiation and development. When *Atf3* is expressed using a *transthyretin* (TTR) promoter, which is specific to endocrine tissue, pancreatic development is disrupted resulting in reduced islet number, or in some cases, a complete lack of islets (Allen-Jennings *et al.*, 2001). There is evidence that mechanistically, ATF3 causes this to occur through regulation of *Pdx1*. *Pdx1* expression is increased in islets during embryonic development, and its expression is maintained in mature islets. Since ATF3 affects *Pdx1* expression, it may also play a role in regulating the cell differentiation process (Piper *et al.*, 2004; Jang, 2011). The role of ATF3 in repressing *Pdx1* transcriptional activity in endocrine tissue alludes to its potential effects in exocrine tissues.

While *Atf3* has been explored in the endocrine pancreas, there is little evidence of its role in exocrine tissue. Studies have identified the effects of ER stress response on acinar cell function, but none have examined the direct effects of ATF3 and its ability to modulate transcriptional activity in this tissue type.

1.6   Rationale, Objectives, Hypothesis

1.6.1   Rationale and Previous Work

PDAC is the most common disease of the pancreas and is difficult to treat and diagnose (Yadav & Lowenfels, 2013; Eser *et al.*, 2014). Patients present with a lack of symptoms until tumour progression has become advanced, leading to a poor prognosis. Pancreatic cancer is the 3rd most common cause of cancer-related death, and incidence continues to rise (Yadav & Lowenfels, 2013; Cid-Arregui & Juarez, 2015; Siegel *et al.*, 2017). Diagnosis of this cancer remains difficult, as there are no specific tests to detect malignancy, and signs and symptoms of this disease can be easily mistaken for other ailments (Cid-Arregui & Juarez, 2015). Current treatment strategies include pancreatic resection followed by systemic chemotherapy, including administration of gemcitabine (Cid-Arregui & Juarez, 2015). However, these protocols show limited efficacy, and over 95% of patients die within 5 years of diagnosis (Yadav & Lowenfels, 2013). Understanding the mechanisms by which patients develop increased susceptibility to cancer following pancreatitis is crucial to develop preventative, diagnostic and treatment strategies.

Uncovering how ATF3 affects ADM development may aid in understanding PDAC initiation and progression. Previous results from our laboratory show that intraperitoneal (I.P.) injection of *Atf3*$^{-/-}$ mice with cerulein leads to increased pancreatic damage and fibrosis 4 hours following injury. However, *Atf3*$^{-/-}$ mice present with healthy acinar tissue following a period of pancreatic regeneration (72 hours following injury) compared to wild type mice, which show increased ADM, fibrosis, and damage. RNA-sequencing

analysis demonstrates that ATF3 affects genetic expression of transcription factors required for pancreatic terminal differentiation, indicating it may be priming injured acinar cells for pathogenic de-differentiation and trans-differentiation. Additionally, the loss of ATF3 is implicated in decreased EGFR signalling following cerulein administration suggesting it may be affecting ADM through this pathway (Fazio *et al.,* 2017). The main goal of my thesis is to understand how ATF3 promotes ADM through either affecting the mature acinar genetic program, or through EGFR signalling.

1.6.2   Hypothesis

I hypothesize that ATF3 regulates acinar gene expression promoting acinar-to-duct cell metaplasia.

1.6.3   Objectives and Significance

1) Determine if factors that regulate acinar cell differentiation are altered in *Atf3*$^{-/-}$ mice
2) Examine the ability for *Atf3*$^{-/-}$ acinar cells to undergo ADM in culture
3) Determine if the absence of ATF3 affects recurrent pancreatic injury

This work aims to determine whether ATF3 is a key regulator of the ADM process. If the mechanism by which ADM develops can be determined, better diagnostic and therapeutics can be established which could aid in blocking the progression to PDAC.

Chapter 2

2   Methods

2.1   Mice

Mice with a germ line deletion of exon 2 within the *Atf3* gene in a C57Bl6 background have been described previously (*Atf3*$^{-/-}$; Hartman *et al.,* 2004). Two-to-four month old mice were used for all experiments and both male and female mice were included. All experiments were conducted with the approval of the Animal Care Committee at the University of Western Ontario following protocol guidelines (#2008-117/2017-001). The genotypes of the mice were confirmed by polymerase chain reaction (PCR) with the following primers: wild-type *Atf3* - 5' TGAAGAAGGTAAACACACCGTG 3'; common *Atf3* - 5' AGAGCTTCAGCAATGGTTTGC 3'; deleted *Atf3* - 5' ATCAGCAGCCTCTGTTCCAC 3'. The PCR program used was 40 cycles of denaturing (95°C for 30 seconds), annealing (63.2°C for 30 seconds), and elongation (72°C for 60 seconds).

To initiate acute pancreatic injury, congenic (inbred) wild-type (*Atf3*$^{+/+}$) or *Atf3*$^{-/-}$ mice were given intraperitoneal (I.P.) injections of saline (vehicle control) or cerulein (Sigma, St. Louis, MO; CIP; 50 μg/kg) once per hour for 4 hours or 8 hours according to a previously established protocol (Kowalik *et al.,* 2007). Ceruelin, a CCK analog, activates CCK receptors and induces pancreatic enzyme release (Aghdassi *et al.*, 2011). Mice were sacrificed at 4 hours or 72 hours following the first injection.

Chronic injury was initiated in the mice by injecting saline (vehicle control) or cerulein I.P. (250 µg/kg) twice daily for 14 days. This protocol was adapted from a previously established protocol (Ardito *et al.,* 2012). Mice were allowed to recover for 7 days before sacrifice. During this time period, mice were weighed once daily (a.m.) to assess changes in body weight.

2.2 RNA Isolation, Polymerase Chain Reaction, and Quantitative Real-Time PCR

Upon dissection, a 2-3 mm^2 splenic portion of the pancreas was removed and placed in TRIzol Reagent (Invitrogen; Carlsbad, CA). A tissue homogenizer was used to break up the tissue for 30 seconds. RNA was isolated using the PureLink^{TM} RNA Minutes Kit (ThermoFisher Scientific, Waltham, MA) as per manufacturer's directions and stored at -80°C. RNA quality was assessed by RNA Integrity analysis using the Bioanalyzer at Roberts Institute at the University of Western Ontario. RNA was quantified using the NanoDrop® ND-1000 UV-Vis Spectrophotometer (ThermoFisher Scientific) and Nanodrop-1000 software.

To perform RT-PCR, RNA was used to generate cDNA through a Reverse Transcriptase reaction using ImProm-II™ Reverse Transcription System (Promega; Madison, WI). Samples were prepared from 1 µg of RNA as per manufacturer's directions. To determine quality of cDNA, PCR was performed using a PCR master mix (10x DreamTaq Green Buffer, DreamTaq DNA polymerase (Thermofisher Scientific) and the appropriate

diluted primers (20 nM), dH$_2$O) for *Mitochondrial Ribosomal Protein* (*Mrpl*) (Table 2.1).
Samples were stored at -20°C.

Quantitative Real Time-Polymerase Chain Reaction (qRT-PCR) was performed using
GoTaq® qPCR Master Mix (Promega, Madison, WI). Primers for genes of interest were
diluted to a final concentration of 20 nM and combined with GoTaq® qPCR Master Mix
and aliquoted (9 µl) to a 365 well plate (see Table 2.1 for primer sequences). qRT-PCR
was performed on 1 µg/µl of cDNA in 9uL of GoTaq® qPCR Master Mix for each
sample in triplicate using the ViiA™ 7 qRT-PCR machine (Applied Biosystems; Foster
City, CA). The program consisted of 40 cycles of denaturing (95°C for 10 seconds),
annealing (see Table 2.1 for temperatures – for 40 seconds), and elongation (72°C for 10
seconds). Results were analyzed using the calibrator normalized method with standard
curves for efficiency correction according to the equation:

Relative amount = $E_T^{\ CpT(C)-CpT(tS)}$ x $E_R^{\ CpR(tS)-CpR(C)}$

Where :

E = Efficiency (E = $10^{-1/m}$; m = slope of standard curve)

Cp = Crossing point (derived by Lightcycler software version 3.5)

T = Target gene (i.e. gene of interest)

R = Reference gene (i.e. housekeeping gene)

C = Calibrator (e.g. saline control)

tS = Sample (e.g. treated sample)

Table 2.1 Primers used for RT-PCR and qRT-PCR

Gene	Annealing Temp (°C)	Fwd	Rev
Mrpl	60	5' TTGGATATGCCAAGTGACCA 3'	5' GCTTCTGCCGTTTGAGTTTC 3'
Nr5a2	60	5' TGGCGATAAAGTGTCTGGGT 3'	5' CCAGCTTCATCCCAACACG 3'
Sox9	60	5' CGTGCAGCACAAGAAAGACCA 3'	5' GCAGCGCCTTGAAGATAGCAT 3'
Krt19	60	5' CCTCCCGCGATTACAACCACT 3'	5' GGCGAGCATTGTCAATCTGT 3'
Pdx1	63	5' CCACCCCAGTTTACAAGCTC 3'	5' TTCAACATCACTGCCAGCTC 3'
Rbpj	63	5' GTGTTCCTCAGCAAGCGGATA 3'	5' TGCCACCTTCGTTCCTGA 3'
Rbpjl	63	5' ATGCCAAGGTGGCTGAGAAAT 3'	5' CTTGGTCTTGCATTGGCTTCA 3'
Egf	63.8	5' ATGTGCCACTCAGAATCACG 3'	5' AAAGTGCAGTCATGGCTGTG 3'
Tgfα	63.8	5' AAGAAGCAAGCCATCACTGC 3'	5' CAAGCAGTCCTTCCCTTCAG 3'
Egfr	60.8	5' CTGCCAAGGCACAAGTAACA 3'	5' GTTGAGGGCAATGAGGACAT 3'
Mek	60.8	5' GGGGAACTGAAGGATGA 3'	5' GGAGTTGCACTCGTGCAGTA 3'

2.3   Protein Isolation and Western Blotting

Protein was isolated from the splenic portion of the pancreas. Tissue was homogenized in 100-500 µl of protein isolation buffer (50 mM Tris [pH 7.2], 5 mM $MgCl_2$, 1 mM $CaCl_2$, 10 mM DTT, 1% NP40, 100 units/ml DNAse I, 50 µg/ml RNAse A, 10 mM PMSF, 5 µg/ml leupeptin, 5 µg/ml aproptinin, 5 µg/ml pepstatin, 50 mM NaF, 2 mM $NaVO_4$ in dH_2O). Following homogenization, tissue was sonicated continuously for 10-20 seconds. Samples were then centrifuged at 4°C for 5 minutes at 5,000g, supernatant was removed and samples were stored at -80°C (Pin *et al.,* 2000).

To isolate protein from primary acinar cells in suspension, media was removed and cells rinsed with cold Phosphate Buffer Solution (PBS). Cells were then centrifuged at 16g for 1 minute to pellet. Cell pellets were mixed with the 100-200 µl of protein isolation buffer (described above), and lysed by pipetting up and down several times. Protein was then processed using the same methods as above.

Protein was quantified using the BioRad protein assay, and absorbance was determined either in duplicate using the Ultrospec 2100 pro UV-visible spectrophotometer (Biochrom, Holliston, MA) at 600 nm or triplicate using the Multiskan Ascent 96/384 Plate Reader (ThermoFischer Scientific) at 595 nm.

To perform Western blot analysis, 2 µg, for amylase analysis, or 40 µg for either pERK or tERK analysis, of protein was mixed with 5 µl of 5x sodium dodecyl sulfate (SDS) loading dye and 1 µl of β-mercaptoethanol, then heated to 100°C for 5 minutes. Samples were resolved on a 10% SDS-polyacrylamide gel at 200V. Protein was transferred to

PVDF membranes (BioRad; Herculus, CA) at 200 mA for 90 minutes. Following

transfer, the membrane was rinsed with PBS and incubated at room temperature for 1

hour in dissolved 5% non-fat dried milk (NFDM) in PBS for 60 minutes. The membrane

was rinsed with either PBS or 0.1% Tween-20 (Dako; Glostrup Municipality, Denmark)

in Tris Buffered Solution (TBS; TBST), depending on the antibody used, 3x for 5

minutes each before incubating with primary antibody. Antibodies against Amylase

(1:1000; Abcam Inc., Cambridge, UK) were diluted in 5% NFDM in PBS, where as

phosphorylated-ERK1/2 (1:500; Cell Signaling Technology, Danvers, MA) and total

ERK (1:250; Cell Signaling Technology, Danvers, MA) were diluted in 5% BSA in

TBST. Membranes were incubated overnight at 4°C with the primary antibody. Prior to

adding the secondary antibody, membranes were rinsed 3x 5 minutes with either PBS

(amylase) or TBST (pERK, tERK). Membranes were incubated in secondary antibody

(anti-rabbit horseradish peroxidase; Sigma 1:10,000) diluted in 5% NFDM in PBS, for 60

minutes at room temperature. Following another set of washes as above, the membranes

were incubated for 2-3 minutes in Clairty Max^{TM} Western ECL Blotting Substrates

(BioRad) at a 1:1 dilution. Blots were visualized using the VersaDoc Imaging System

with Quantity One 1-D Analysis software (BioRad).

In some instances, the membrane was stripped of primary antibody prior to reprobing.

The membrane was incubated with stripping buffer solution (100 mM 2-mercaptoethanol,

62.5 mM Tris HCl [pH 6.7], 2% sodium dodecyl sulfate in dH$_2$O) for 30 minutes at 55°C,

and was then rinsed with TBS, before washing with TBST for 7 minutes. The membrane

was washed 2 x 5 minutes each with TBS before adding 5% NFDM in PBS blocking

solution for 60 minutes. The membrane was processed following the same protocol as described above.

2.4   Acinar Cell Isolation and Culture

To establish acinar cell cultures, fresh pancreata from 2-4 month old male and female wild type and *Atf3*^{-/-} mouse were dissected and immediately incubated in DMEM media (Gibco, ThermoFisher Scientific) supplemented with 1% Penstrep and 0.1% soybean trypsin inhibitor, previously diffused with oxygen (oxygenation) for 20 minutes. Oxygenation occurs by bubbling oxygen from an oxygen tank through media using a glass pipette. Pancreatic tissue was repeatedly injected with DMEM containing collagenase (200 µL of 1000U/10 ml) using a 1 mL syringe and 26.5 gauge needle. Once the pancreas was distended, it was cut into smaller pieces oxygenated for 1 minute, then rocked at 120 oscillations per minute in a 37°C incubator for 10 minutes. The DMEM-collagenase solution was replaced with fresh solution, and oxygenation repeated for an additional 40 minutes. The tissue homogenate was disrupted further by pipetting though a 10 mL, then 5 mL serological pipette. Homogenates were strained though a 105 µm nylon mesh filter. The nylon filter was washed with DMEM containing 4% Bovine Serum Albumin Fraction V (BSA; Roche, Basel, Switzerland). At this point, the tissue homogenate consisted of individual, or small clumps of acini. The tissue homogenate was divided into 4 samples, and each centrifuged at 45g for 3 minutes to pellet the acini. The supernatant was removed, and acini washed with 40 mL of DMEM+4% BSA. Acini were pelleted as described above, and 2 subsequent washes were repeated with DMEM

containing 1% BSA. Acini were combined to one tube, and incubated at 37°C for 15 minutes.

Acini were cultured in RPMI media (Gibco, ThermoFisher Scientific, supplemented with 1% Penstrep, 1% Newborn Calf Serum (NCBS), 0.1% soybean trypsin inhibitor and 1% dexamethasone) overnight for protein isolation, or embedded in collagen. To embed acini in collagen, supernatant was removed and acini were resuspended in a 1:1 ratio of RPMI media and Rat Tail Type 1 Collagen (3.68 mg/ml; Corning, Corning, NY). Neutralization buffer (2:3 ratio of 0.34 M NaOH and 10x Waymouth Media) was added drop wise to the acini and collagen solution under mild vortexing. Acini were plated in 3 cm dishes (400 µL per dish) and incubated at 37°C until collagen solidified. RPMI media (2 mL) was added and media was replaced the following day, and subsequently every other day. Cultures were treated with 0.1% BSA in PBS or 50 ng/mL of TGFα (diluted in 0.1% BSA in PBS) on the day of isolation, then the 1 and 3 days following isolation.

2.5   Tissue Fixation and Staining

Tissues from the body and neck of the pancreata from mice were isolated and fixed in 4% paraformaldehyde or Shandon cryomatrix embedding resin (ThermoFisher Scientific) for paraffin or cryostat sectioning, respectively. Paraffin sections were embedded following rehydration. Paraffin and cryostat samples were sectioned to 5-7 µm using the HM325 Rotary Microtome (ThermoFisher Scientific) or the Shandon cryostat (ThermoFisher Scientific), respectively.

Acini embedded in collagen matrices were fixed in cryomatrix after one or three days of culture with 4% formaldehyde in PBS overnight. The following day, samples were rinsed with PBS 3x 1 hour each, and 5% sucrose solution was added. Samples were incubated overnight. Over two subsequent days, samples were transferred to 10% and then 20% sucrose solutions. Cells were embedded in Shandon Cryomatrix resin and sectioned to 5-8 μm using the Shandon cryostat.

For immunofluorescence (IF) analysis, cryostat tissue sections were fixed in 4% formaldehyde in PBS for 10 minutes, then washed 3 x 5 minutes in PBS. Sections were permeabilized in 0.1% Triton X-100 in PBS for 10 minutes, followed by 3 x 5 minutes PBS washes. Tissue was incubated in blocking solution consisting of 5% BSA in 0.1% Triton X-100 in PBS, and incubated at room temperature for 30 minutes. Sections were washed with blocking solution 3 x 5 minutes before adding primary antibody diluted in blocking solution and incubated at 4°C overnight. The primary antibodies used were ones raised against amylase (1:1000; Abcam Inc.). Slides were washed 3 x 5 minutes with PBS before adding anti-rabbit fluorescein isothiocyanate (FITC;1:250, Jackson ImmunoResearch, West Grove, PA) diluted in blocking solution for 1 hour at room temperature. To allow for visualization of nuclei, sections were incubated for 5 minutes in 4',6-diamidino-2-phenylindole (DAPI; 1:1000) diluted in dH$_2$O. Slides were washed 3 x 5 minutes with dH$_2$O and mounted using PermaFluor mounting media (ThermoFisher Scientific). Tissue sections were imaged using an Automated Upright Microscope (Leica Microscope DM5500B, camera DFC450; Leica Microsystems, Wetzlar, Germany) and LAS V4.4 software (Leica Microsystems).

For immunohistochemical (IHC) analysis, paraffin slides were dehydrated through a xylene/ethanol series and then immersed in working solution (0.1 M Citric Acid Monohydrate, 0.1 M sodium citrate dehydrate in dH$_2$O) and boiled for 45 minutes for antigen retrieval. Sections were cooled to room temperature (~20 minutes). Tissue was processed using the Immunocruz Rabbit ABC Staining System (Santa Cruz, Dallas, TX). Briefly, sections were incubated in a methanol, hydrogen peroxide solution for 10 minutes, permeabilized in 0.2% Triton X-100 in PBS for 12 minutes, then washed with 0.2% Tween-20 in PBS for 5 minutes. Sections were incubated in blocking solution (5% rabbit serum and PBS) for 1 h before incubating in primary antibody raised against SOX9 (1:500, diluted in blocking solution, Abcam Inc., Cambridge, United Kingdom) overnight at 4°C. The following day, sections were rinsed with 0.2% Tween-20 in PBS for 6 minutes, followed by 4 x 6 minutes PBS washes. Sections were then incubated at room temperature for 30 minutes with biotinylated mouse anti-rabbit IgG secondary antibody (diluted 1:1000 as per manufacturer's instructions) (Sigma). Sections were washed for 6 minutes with 0.2% Tween-20 in PBS, then 2 x 6 minutes with PBS. Sections were incubated for 30 minutes in AB enzyme reagent (avidin, biotinylated HRP, PBS), prepared as per Immunocruz Rabbit ABC staining system directions. Sections were washed 3 x 6 minutes each with PBS, incubated in Peroxidase substrate for 6-20 minutes, until nuclei staining was visible on positive controls. Sections were washed 3 x 5 minutes in dH$_2$O, then counterstained with hematoxylin for 1 minute, followed by dehydration through ethanol/xylene.

For histological examination of tissues, sections were stained with hematoxylin and eosin (H&E) and Masson's Trichrome. For paraffin tissue sections, slides were deparaffinized

in xylene 3 x 5 minutes, then rehydrated through ethanol and dH$_2$O. For frozen cell

sections, the previous steps were omitted, and slides were placed directly into 70%

ethanol for 2 minutes. Slides were then stained with H&E. Tissue was subsequently

dehydrated in 90% ethanol for 1 minute, then 100% ethanol 2x for 3 minutes, before

being placed in xylene 3x for 5 minutes. Paraffin tissue sections were stained for

Masson's Trichrome using kit instructions. Following staining, slides were mounted

using Permount and imaged using an Automated Upright Microscope (Leica Microscope

DM5500B, camera DFC450 FX) and LAS V4.4 software (Leica Microsystems).

2.6 Cyst, Cell Thickness and Lesion Area Quantification

To assess acinar-to-duct cell metaplasia in culture, acinar cell clusters were visually

assessed on days 1 and 3 following isolation using an inverted, phase-contrast

microscope (Leica DMIL). Culture in 3D collagen matrix allows for cysts to develop in

multiple planes of focus. For these in vitro studies, I established a set of criteria to

identify ADM structures: i) a lumen had to appear in a cluster of acinar cells, ii) be

visible in multiple planes of focus, iii) and appear with flattened cellular structures

surrounding it. To capture the entirety of the plate, 50 acinar cell clusters were counted,

and ADM quantified.

Cell thickness, of acinar cells that make up putative ADM in TGFα-treated cultures, was

analyzed on paraffin sections stained with H&E, and assessed using ImageJ software.

Cell thickness was determined according to the width of the nuclei surrounding the

perimeter of putative ADM. Nuclei were measured at 3 distinct, evenly spaced points

around the structure (**Appendix 1**). An average of 3 measurements per cyst were

calculated, for 1-6 cysts per genotype on days 1 or 3 of culture. Data presented is the average of three wild type and three $Atf3^{-/-}$ mice.

To assess the degree of damage and inflammation present in pancreatic tissue, H&E slides were imaged using the Aperio CS2 Digital Scanner and Aperio Imagescope Software (Leico Biosystems Imaging Inc.) Images were then analyzed using ImageJ (National Institutes of Health, Maryland, USA) software to determine the area of damage and inflammation (lesion area) relative to total tissue area.

2.7   Statistical Analysis

Differences between experimental groups for cell culture analysis, as well as body weight analysis for the chronic pancreatitis experiment were compared using a repeated measures two-way ANOVA, followed by Tukey's post hoc test. QRT-PCR results were analyzed using an unpaired t-test, with the exception of $Rbpj/Rbpjl$ ratio, which were analyzed by two-way ANOVA, followed by Tukey's post hoc test. Western blots and lesion area quantification were analyzed by an unpaired t-test. Significance is considered a P-value <0.05.

Chapter 3

3   Results

3.1 *Atf3* promotes gene expression changes indicative of ADM development

Previous work suggested that loss of ATF3 resulted in reduced ADM *in vivo* (Fazio *et al.,* 2017). To determine the underlying mechanisms, congenic wild-type ($Atf3^{+/+}$) and $Atf3^{-/-}$ mice were treated with cerulein, and analyzed 4 and 72 hours after initial injections. Expression of RBPJ and RBPJL*,* both of which compete for binding to the PTF1A complex, were assessed as markers of a de-differentiated (progenitor-like) and differentiated (acinar) phenotype, respectively. At 4 hours post-CIP, *Rbpj* mRNA levels were significantly increased in pancreatic tissue of wild-type mice (2.16±0.34 fold), while *Rbpjl* mRNA levels was not statistically different (p>0.05) compared to saline. Conversely, pancreatic tissue from $Atf3^{-/-}$ mice showed no changes in either *Rbpj* or *Rbpjl* mRNA levels at 4 hours post-CIP (p>0.05; **Figure 3.1A**). At 72 hours post-CIP, mRNA levels of *Rbpj* remained significantly higher in CIP-treated wild-type mice (6.04±1.01 fold), while *Rbpjl* was unchanged from saline-treated controls. Similar comparisons in $Atf3^{-/-}$ mice at 72 hours post-CIP revealed significantly increased *Rbpj* mRNA levels (3.74±0.80 fold), with no changes in *Rbpjl* mRNA levels compared to saline-treated controls (p>0.05; **Figure 3.1A**). Since RBPJ and RBPJL compete for PTF1A, we examined the ratio of the mRNA levels of the two genes following CIP (Masui *et al.*, 2010). At 4 hours post-CIP, the ratio of *Rbpj/Rbpjl* was significantly increased in both wild-type and $Atf3^{-/-}$ mice when compared to saline treatment

A.

Rbpj

4 hours

72 hours

Rbpjl

4 hours

72 hours

B.
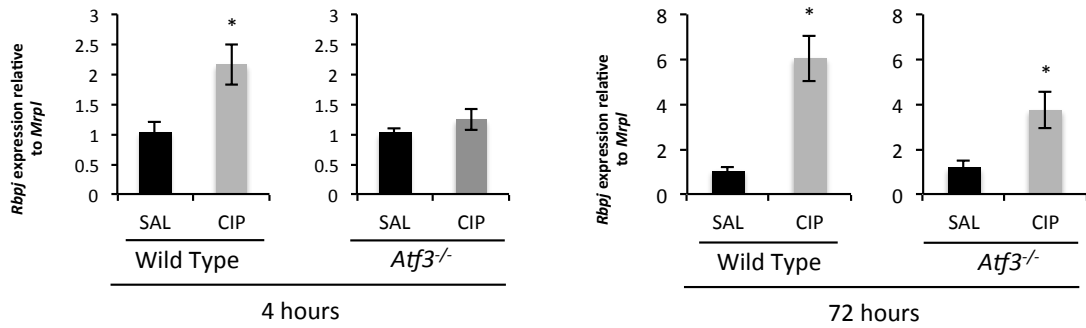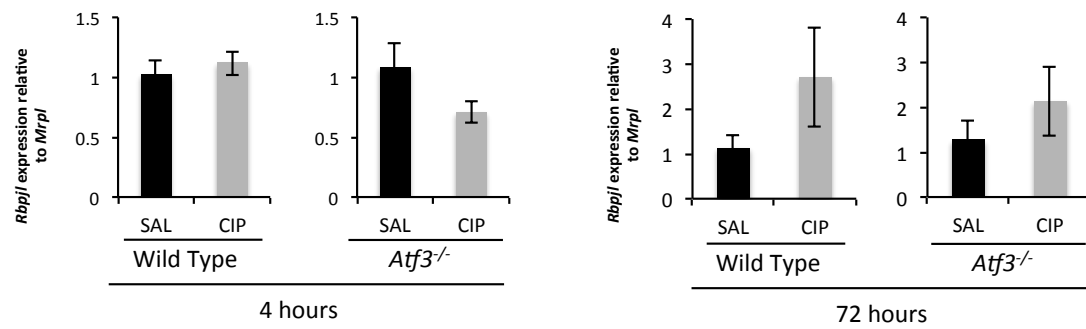
Rbpj/ Rbpjl
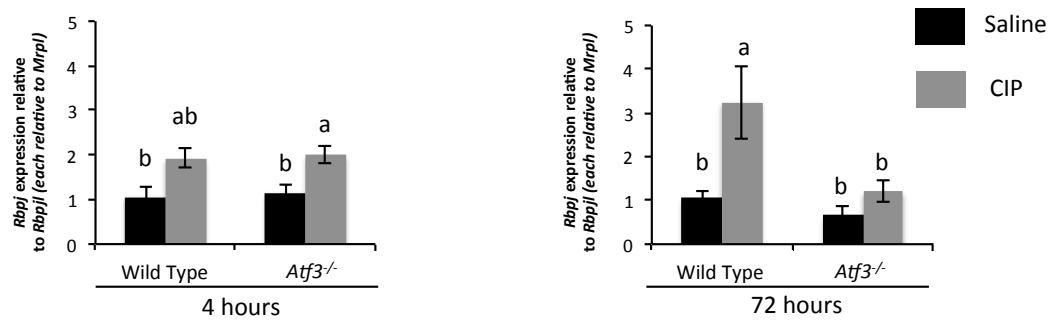
4 hours

72 hours

Figure 3.1 *Atf3*^{-/-} **mice show altered ratios of *Rbpj* and *Rbpjl* gene expression during acute CIP. (A)** QRT-PCR analysis of *Rbpj* and *Rbpjl* expression in pancreatic tissue from wild type and *Atf3*^{-/-} mice at 4 and 72 hours following saline (SAL) or cerulein (CIP) treatment. *Rbpj* expression was significantly increased in wild-type mice at both 4 and 72 hours post-CIP compared to saline, while in *Atf3*^{-/-} mice, *Rbpj* was only elevated at 72 hours post-CIP compared to saline (*p<0.05). *Rbpjl* expression was not statistically different compared to saline for either genotypes at 4 or 72 hours post CIP (p>0.05). **(B)** When assessed as a ratio of *Rbpj* to *Rbpjl*, both relative to *Mrpl*, *Rbpj*/*Rbpjl* expression was significantly increased in wild type and *Atf3*^{-/-} 4 hours post-CIP compared to saline, and only in wild-type tissue 72 hours post-CIP compared to saline (^ap<0.05; n=4-6). Mean±SEM is shown.

(p<0.0001). This effect was maintained in wild-type mice at 72 hours, where CIP-treated mice showed a significantly increased ratio compared to all groups. In contrast, no changes were detected in the ratio of *Rbpj/Rbpjl* in *Atf3*$^{-/-}$ mice at 72 hours post CIP (p<0.0001; **Figure 3.1B**). This suggests loss of *Atf3* does not alter progenitor mRNA levels to affect the ADM phenotype.

I next assessed expression of *Nr5a2*, a marker of acinar cell maturation. In wild-type mice, expression of *Nr5a2* was significantly decreased 4 hours following CIP treatment (0.68±0.05 fold), but was not significantly different 72 hours following treatment (p>0.05; **Figure 3.2**) compared to saline-treated mice. Comparatively, *Nr5a2* expression was not different in *Atf3*$^{-/-}$ mice at either time point, suggesting ATF3 may not be targeting *Nr5a2* expression following initial injury (p>0.05).

MRNA levels of genes that represent a progenitor-like phenotype, and are re-activated during ADM, were assessed by qRT-PCR analysis. *Pdx1* exhibited no changes in expression following CIP at either time point in both genotypes (**Figure 3.3A**). Conversely *Sox9* expression was significantly increased in pancreatic tissue from wild-type mice at both 4 (6.17±1.23 fold) and 72 hours (4.95±0.85 fold) following CIP (**Figure 3.3B**) compared to saline. Similar analysis in pancreatic tissue from *Atf3*$^{-/-}$ mice revealed a significant increase in *Sox9* expression only at 4 hours (2.41±0.28 fold) following injury, but not at 72 hours post CIP (p>0.05). These results suggested that ATF3 may be required for increased *Sox9* expression and increased progenitor gene expression during ADM.

Nr5a2
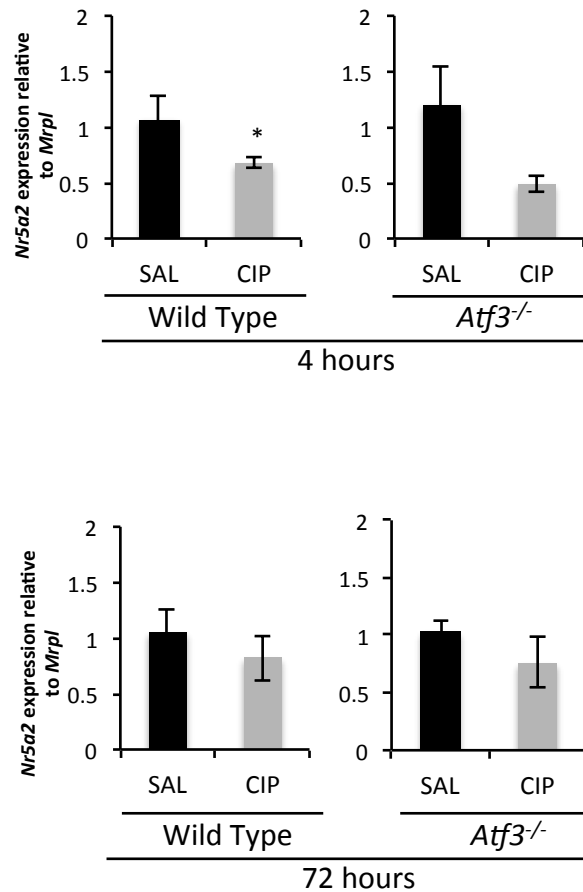
Figure 3.2 Wild type mice show decreased *Nr5a2* expression during acute CIP. QRT-PCR analysis of *Nr5a2* expression 4 and 72 hours after saline (SAL) and cerulein (CIP) treatment. *Nr5a2* was significantly decreased 4 hours post-CIP in wild-type mice compared to saline treated mice ($^*p<0.05$), while there was no statistical difference for *Nr5a2* 72 hours post-CIP (n=4-6) compared to saline. No statistical difference was observed in *Atf3^{-/-}* models 4 and 72 hours following CIP compared to saline (n=4-6; $p<0.05$). Mean±SEM is shown.

A.

Pdx1
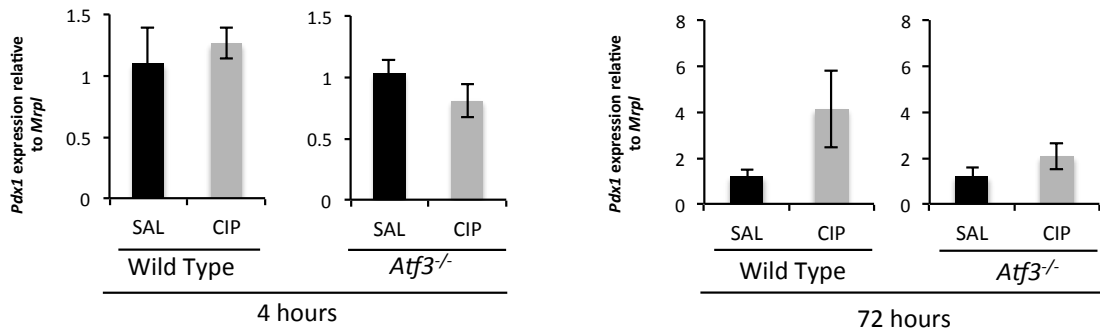
B.

Sox9
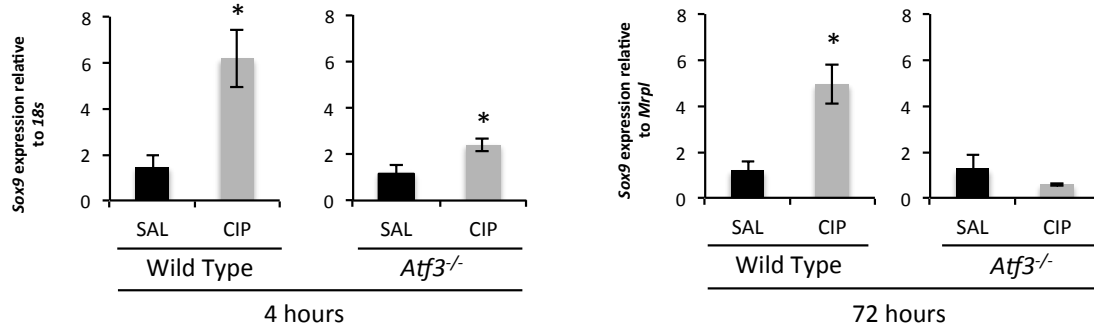
C.

Krt19
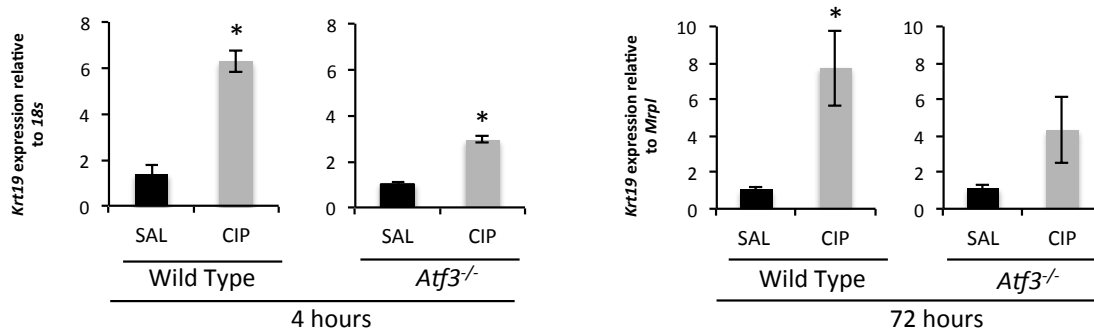
Figure 3.3 Wild type mice show increased gene expression of pancreatic progenitor and duct markers at later time points in acute CIP (A) QRT-PCR analysis of *Pdx1* expression at 4 and 72 hours after saline (SAL) or cerulein (CIP) treatment indicated no significant difference in wild type and *Atf3*$^{-/-}$ ($p > 0.05$) compared to saline controls. QRT-PCR analysis of **(B)** *Sox9* and **(C)** *Krt19* at 4 and 72 hours following CIP. Expression of *Sox9* and *Krt19* was significantly increased in pancreatic tissue at 4 hours post-CIP in both wild-type and *Atf3*$^{-/-}$ compared to saline, however expression remained significantly increased at 72 hours compared to saline in only CIP-treated wild-type mice ($^{*}p < 0.05$; n=4-6). Mean±SEM is shown.

To assess the effect of *Atf3* on the expression of a specific duct cell marker, qRT-PCR

was performed for *Krt19* (**Figure 3.3.C**). Expression of *Krt19* was significantly increased

in wild-type mice following CIP at both time points (4 hours, 6.29±0.46 fold; 72 hours,

4.30±1.81 fold) compared to saline (**Figure 3.3C**). However, *Krt19* expression was only

increased in *Atf3*$^{-/-}$ CIP-treated mice at 4 hours (2.94±0.15 fold), and not at 72 hours post

CIP (p>0.05), suggesting ATF3 was required for ductal marker expression. Alternatively,

ATF3 may be responsible for promotion of a progenitor phenotype, thereby allowing

ductal differentiation to occur. To confirm that SOX9 expression was specific to ADM, I

performed IHC and showed that 72 hours following injury, SOX9 accumulated in

lesioned areas (pancreatic tissue with damage and evidence of ADM) in wild-type mice

(**Figure 3.4**). While some SOX9 expression was observed in pancreatic tissue from *Atf3*$^{-/-}$

mice, this accumulation of SOX9 was reduced compared to wild type CIP-treated models

and found mostly in putative acinar cells (**Figure 3.4**).

Signaling through the EGFR pathway is required for ADM development (Ardito *et al.*,

2012; Eser *et al.*, 2014). To determine if ATF3 was promoting ADM development by

affecting EGFR signaling, mRNA expression of *Egfr* and a downstream regulator of the

pathway, *Mek1*, was assessed (**Figure 3.5A**). *Egfr* expression was significantly increased

in pancreatic tissue from wild-type mice at both 4 (8.27±0.66 fold) and 72 (6.29±0.93

fold) hours following CIP compared to saline, while *Atf3*$^{-/-}$ mice showed increased *Egfr*

expression only 4 hours following CIP compared to saline (4.66±1.03 fold) (**Figure

3.5A**). Increased *Mek1* expression is observed 4 (1.94±0.18 fold) and 72 (5.86±1.27 fold)

hours following injury in wild-type mice compared to saline, but not at either time point

in *Atf3*$^{-/-}$ mice (p>0.05; **Figure 3.5B**). Analysis of EGFR ligands 4 hours post-CIP shows
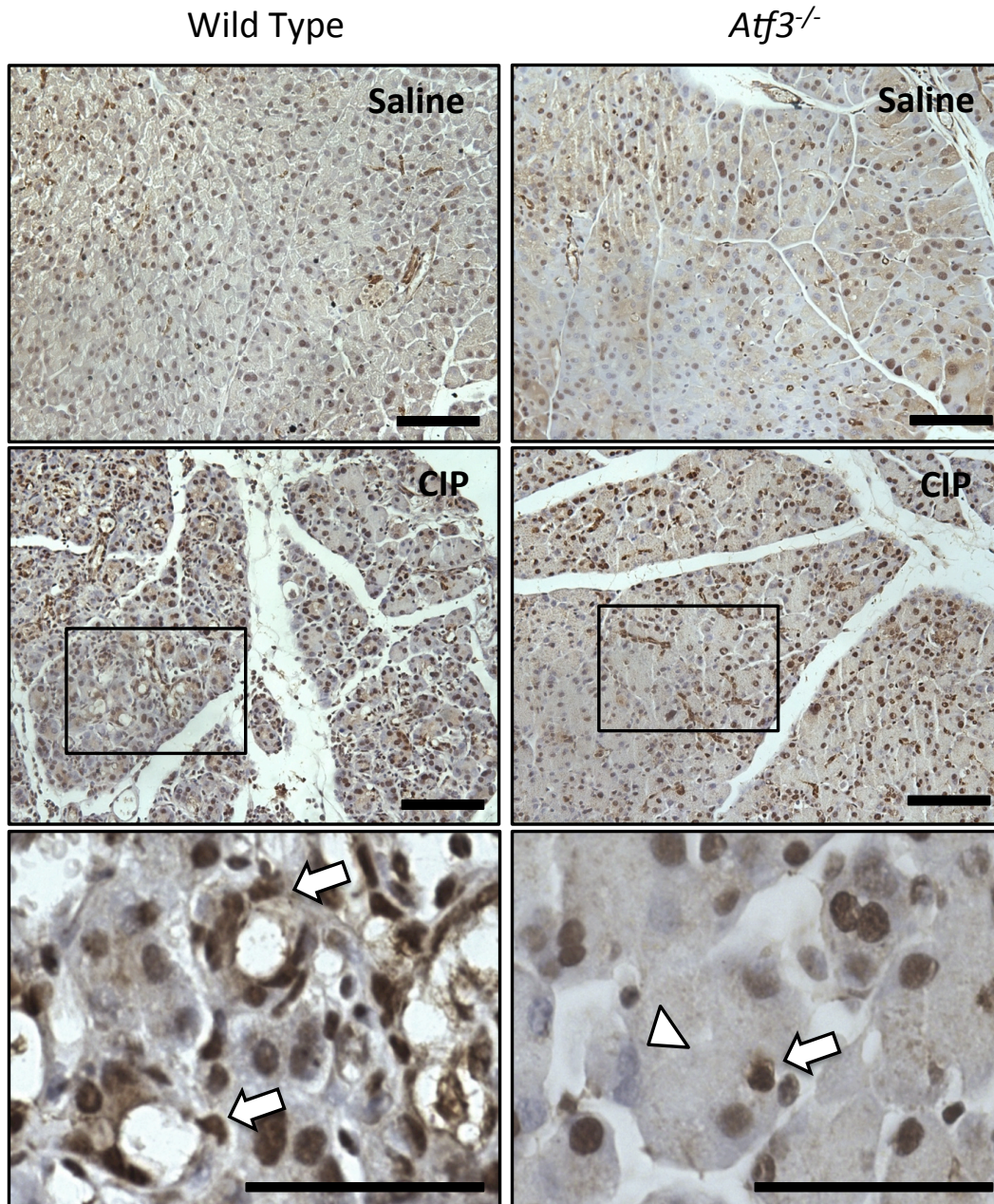
Figure 3.4 SOX9 accumulation occurs in ADM lesions in wild type pancreatic tissue.
(A) Immunohistochemical analysis for SOX9, a pancreatic progenitor marker, shows more positive staining of SOX9$^+$ cells (white arrows) in wild-type tissue following CIP relative to tissue from *Atf3*$^{-/-}$ mice at the same time point. White arrowheads indicate no SOX9 expression. Black boxes indicate regions of higher magnification. Scale bars = 50 μm.

A.

Egfr

4 hours

72 hours

B.

Mek1

4 hours

72 hours

C.

Egf

Tgfα

4 hours

4 hours
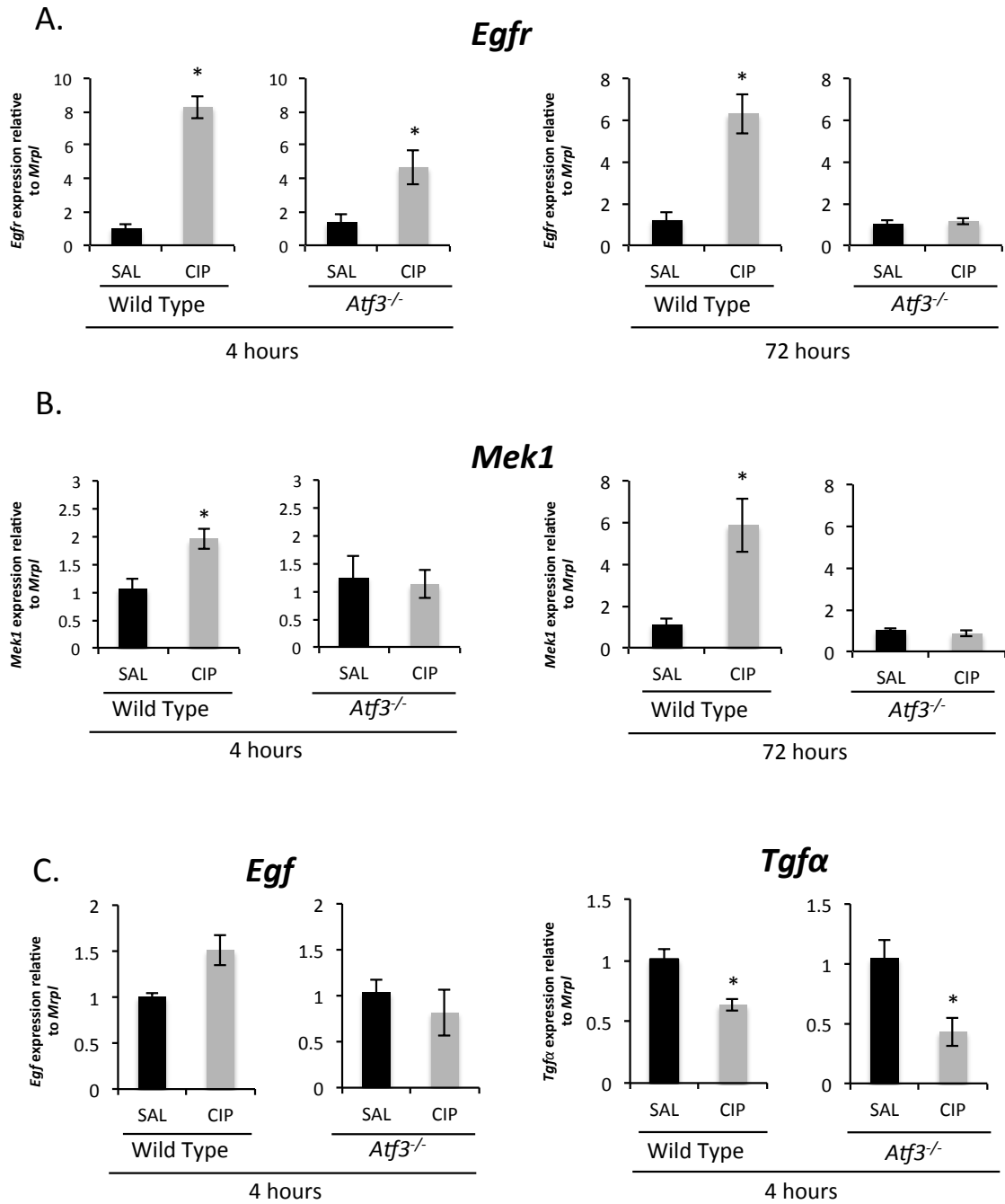
Figure 3.5 Absence of ATF3 affects mRNA levels of EGFR signalling pathway members and ligands during acute CIP. QRT-PCR analysis of EGFR pathway members **(A)** *Egfr* and **(B)** *Mek1* following saline (SAL) or cerulein (CIP) treatment. Increased expression of *Egfr* compared to saline was detected at both 4 and 72 hours post-CIP in pancreatic tissue of wild-type mice. *Atf3*^{-/-} mice show significantly increased expression of *Egfr* at 4 hours, but not 72 hours (p>0.05), post-CIP compared to saline. *Mek1* expression is significantly increased at 4 and 72 hours following injury in wild-type mice (p<0.05), with no statistically difference in *Mek1* expression in *Atf3*^{-/-} mice post-CIP at either time point compared to saline (p>0.05; n=4-6). **(C)** QRT-PCR assessment of EGFR ligands *Egf* and *Tgfα* show significantly decreased expression of *Tgfα* in both wild-type and *Atf3*^{-/-} mice 4 hours post-CIP compared to saline (p<0.05); however, no statistical differences in *Egf* expression was detected in mice of either genotype following CIP at the same time point (p>0.05; n=4-6). Mean±SEM is shown.

a significant decrease in *Tgfa* expression following CIP in both wild-type (0.64±0.05 fold) and *Atf3*^{-/-} mice (0.43±0.12 fold) compared to saline; however no significant differences following cerulein treatment compared to saline were detected in the expression of *Egf* (p>0.05; **Figure 3.5C**).

To see if the changes in mRNA expression were reflective of changes to EGFR pathway protein abundance, the ratio of active ERK (pERK) to total ERK was assessed at 4 hours post- CIP. pERK/tERK ratio in wild type and *Atf3*^{-/-} mice was compared relative to saline (**Figure 3.6A**). As insufficient n values did not allow for statistical analysis, comparisons were made between only cerulein-treated samples. While the ratio of pERK to tERK seemed higher in CIP-treated wild-type mice, the increase was not significant when compared to samples from CIP-treated *Atf3*^{-/-} mice (p>0.05; **Figure 3.6B**). The variability in these findings may reflect the low number of mice included in this analysis (n=3).

3.2 *Atf3*^{-/-} acini form morphologically distinct structures compared to wild type acini in culture

During CIP, ATF3 appeared to be required for changes in gene expression that prime cells for acinar cell de-differentiation, and promote transdifferentiation to a more duct-like phenotype. To determine if the ability to undergo ADM is dependent on ATF3 expression, acinar cells from wild-type and *Atf3*^{-/-} mice were isolated and treated with TGFα, a ligand for EGFR signaling known to be involved in ADM development (Means *et al.,* 2005; Shi *et al.,* 2013; Liou *et al.,* 2015). Cultured cells were embedded in collagen, either left untreated, treated with a vehicle (BSA) or 50 ng/mL TGFα, and followed for 3 days post-isolation (**Figure 3.7A**). Cysts (putative ADM) were counted for a total of 50 acinar clusters per

A.

4 hours

Wild Type   *Atf3*⁻/⁻

SAL SAL CIP CIP   SAL SAL CIP CIP

pERK

tERK

B.

4 hours

WT CIP   *Atf3*⁻/⁻ CIP
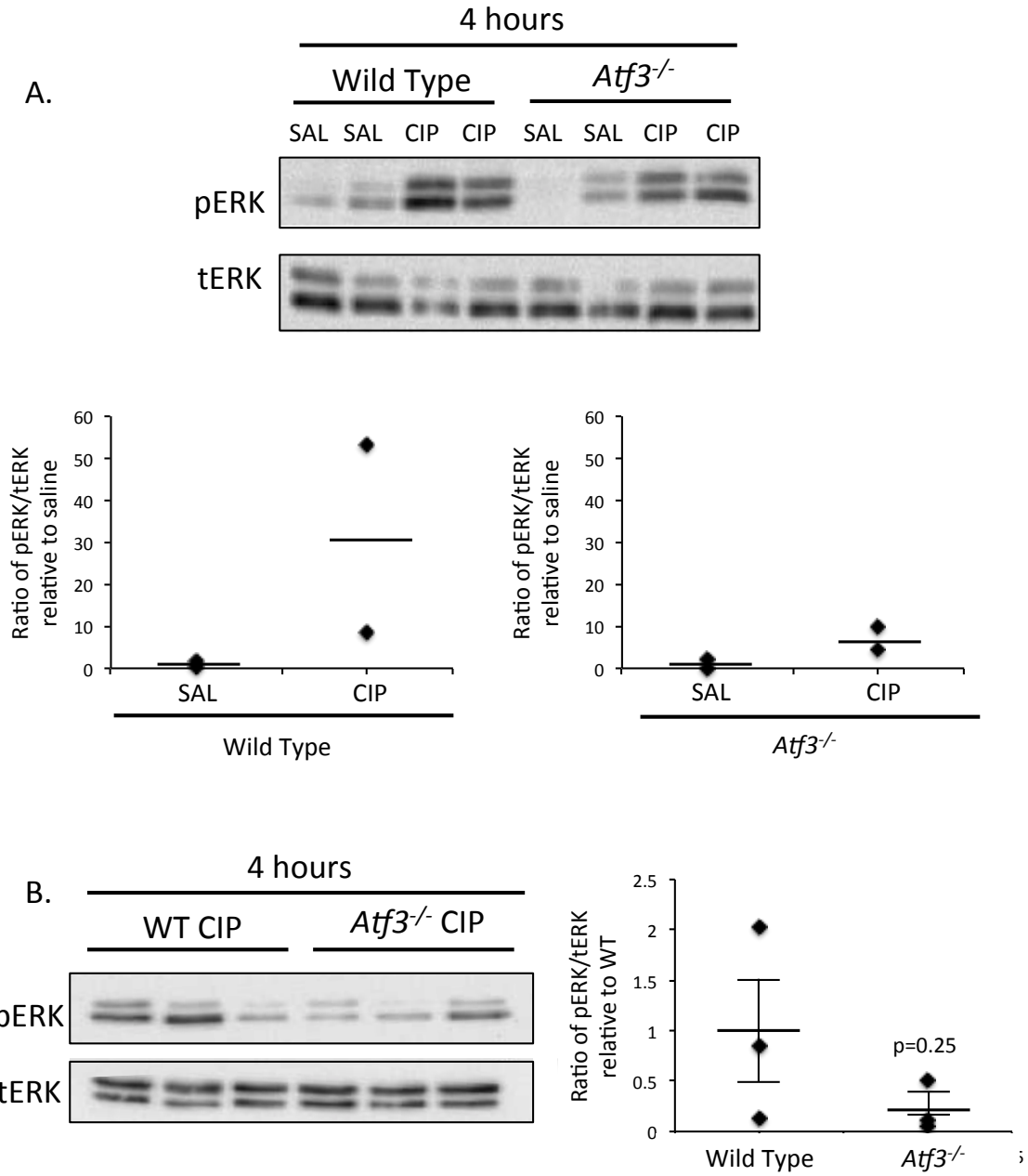
pERK

tERK

Figure 3.6 Loss of ATF3 does not affect EGFR pathway protein abundance

(A) Western blot analysis of phosphorylated ERK (pERK) levels relative to total ERK (tERK) in pancreatic tissue of wild-type and *Atf3*$^{-/-}$ mice 4 hours following saline and CIP treatment. No statistical analysis was completed due to insufficient n values (n=2). **(B)** Western blot analysis of pERK levels relative to tERK for only CIP-treated tissue indicates no statistical difference in ERK abundance in *Atf3*$^{-/-}$ tissue relative to wild-type tissue (p=0.25; n=3). Mean±SEM is shown.

A.

Wild Type

	Day 1	Day 2	Day 3
unt			
BSA			
TGFα			

Atf3⁻ᐟ⁻

	Day 1	Day 2	Day 3
unt			
BSA			
TGFα			

B.

Legend:
- Wild type unt
- Wild type BSA
- Wild type TGFα
- *Atf3⁻ᐟ⁻* unt
- *Atf3⁻ᐟ⁻* BSA
- *Atf3⁻ᐟ⁻* TGFα
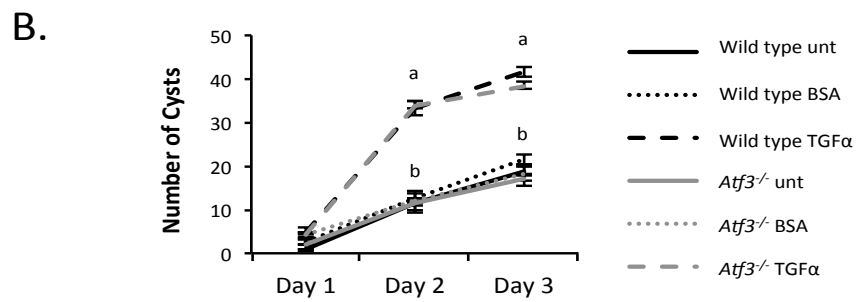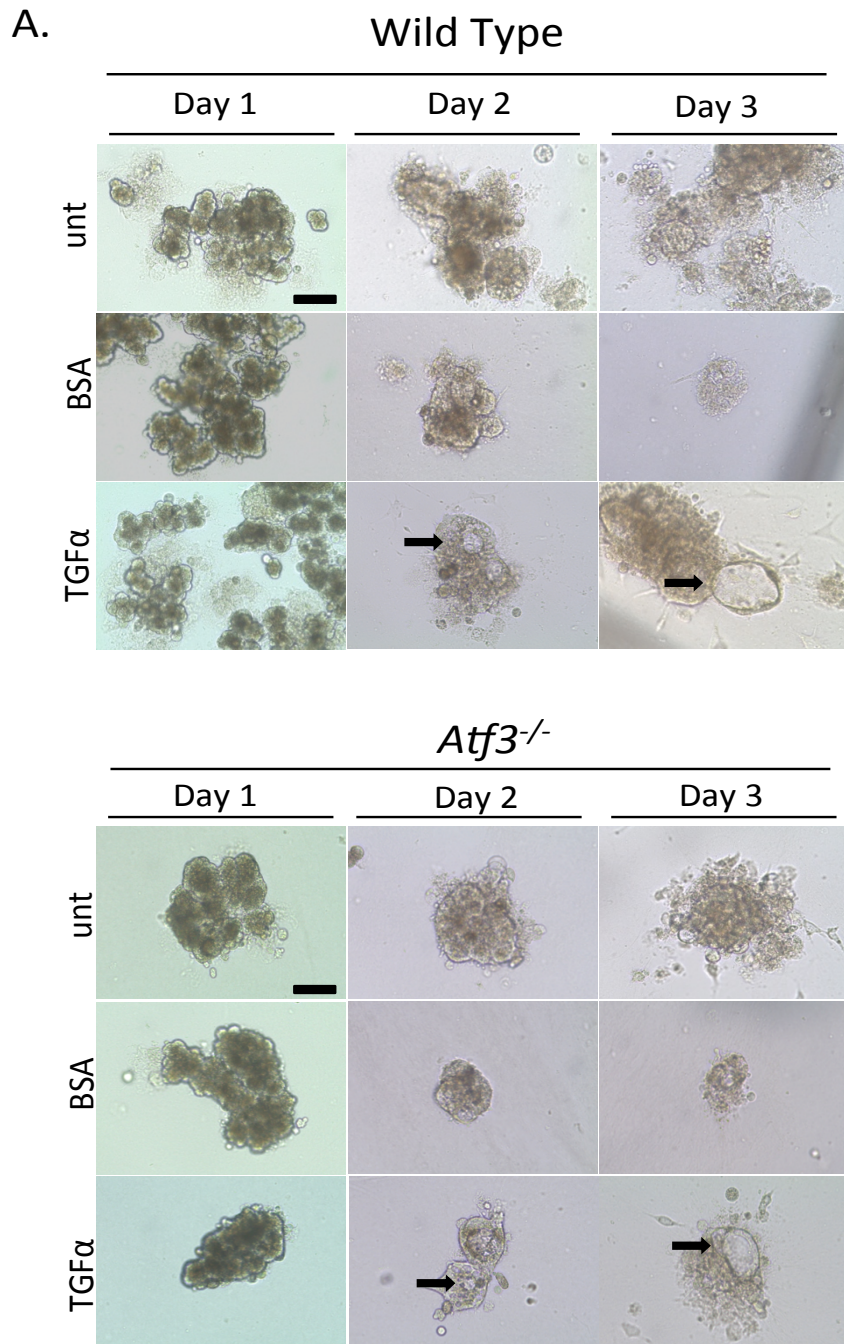
Figure 3.7 Morphology of wild-type and *Atf3*^{-/-} acini cysts following TGFα treatment.

(A) Representative bright field images for wild-type (WT) and *Atf3*$^{-/-}$ untreated (unt) acini, or acini treated with 0.1% bovine serum albumin (BSA) in PBS or 50 ng/mL TGFα and cultured for 1-3 days. Cysts (black arrows) are observed in both WT and *Atf3*$^{-/-}$ TGFα-treated acini by day 2 and 3. Scale bars= 100 μm.

(B) Quantification of the number of cysts found in 50 acinar cell clusters isolated from WT and *Atf3*$^{-/-}$ mice for untreated, and BSA and TGFα treated cells. Both wild type and *Atf3*$^{-/-}$ cells treated with TGFα produce significantly more cysts than untreated and BSA controls (^{a}p>0.05), however no statistical significance is observed between wild-type and *Atf3*$^{-/-}$ cells in any treatment group (n=4). Mean±SEM is shown.

treatment group. Untreated and BSA-treated cells formed cysts (putative ADM) in less than 20% of the total acinar clusters in cells isolated from both wild-type (unt=10.44 cysts; BSA=12.11 cysts) and $Atf3^{-/-}$ (unt=10.22 cysts; BSA=11.33 cysts) mice.

Significantly more cysts formed in wild-type cells (26.56 cysts/50 acinar clusters) treated with TGFα (p<0.05) compared to controls. Analysis of cyst formation in $Atf3^{-/-}$ cultures showed similar results (25.56 cysts/50 acinar clusters), indicating ATF3 is not necessary for TGFα-mediated cyst formation in culture (**Figure 3.7B**).

Analysis of the cysts suggested a difference in morphology between wild type and $Atf3^{-/-}$ acini. Sections of acinar cell cultures were examined by H&E staining to compare overall morphology. At day 3, wild-type acinar clusters treated with TGFα formed putative ADM structures that showed a squamous (thin and flattened)-cell like morphology (**Figure 3.8A**). Conversely, $Atf3^{-/-}$ cultures did form cyst structures, but were less squamous-cell like, as the perimeter of the acinar cell, and the nuclei within it, were not elongated as seen in wild type cells. Quantitatively, at day 3 in culture, ADM structures from wild-type pancreatic tissue had significantly thinner cells (6.19 ± 0.50 μm vs. 9.22 ± 0.41 μm) composing the perimeter, indicating a more squamous-cell phenotype relative to $Atf3^{-/-}$ cysts which had thicker cells composing the perimeter (p<0.05; **Figure 3.8B**).

Cell thickness alone does not indicate whether ADM that forms between these two genotypes are phenotypically different. Therefore it was necessary to stain for a mature acinar cell marker. BSA and TGFα-treated acinar cells from wild-type and $Atf3^{-/-}$ mice were stained against amylase by immunofluorescence. Positive amylase staining was

A.
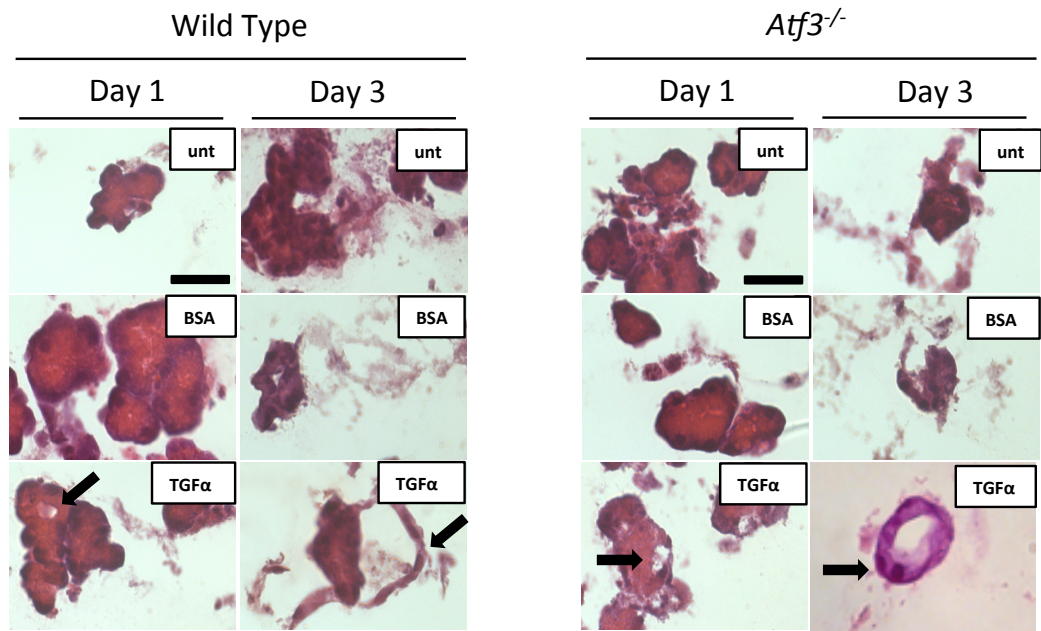
B.
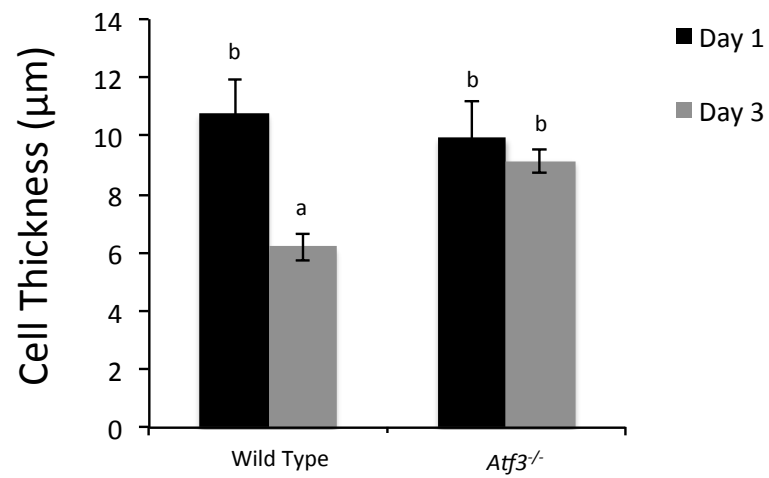
Figure 3.8 *Atf3^-/-* acini form morphologically distinct cysts from wild-type acini.
(A) Representative H&E staining of untreated (unt), and BSA and TGFα treated wild-type (WT) and *Atf3^-/-* acini cultured for 1-3 days. Cysts (black arrows) are observed in both WT and *Atf3^-/-* TGFα-treated acini by day 3. Scale bars = 100 μm. **(B)** Quantification of cell thickness in cysts of TGFα-treated acinar cells on days 1 and 3. By day 3, wild-type acinar cells have significantly thinner cells around the perimeter of the cyst, indicating a more squamous-like phenotype ([a]$p<0.05$; n=1-6 cysts per treatment condition. This was repeated for 3 wild-type and 3 *Atf3^-/-* mice). Mean±SEM is shown.

observed in wild-type cells at day 1, while decreased staining was observed diminished by day 3 following TGFα treatment. Similar analysis of $Atf3^{-/-}$ cultures showed positive amylase staining at day 1 that was maintained on day 3, including following TGFα treatment. This suggests that while ADM-like structures were present in $Atf3^{-/-}$ cultures, these cells did not lose a mature acinar differentiation status (**Figure 3.9**).

3.3 $Atf3^{-/-}$ mice show decreased severity of acinar tissue damage in response to recurrent pancreatic injury

Findings thus far suggested that absence of $Atf3$ altered the ADM process both *in vivo* following acute injury, and *ex vivo* in culture. These results suggested that loss of ATF3 would affect the response to chronic or recurrent pancreatic injury, which is a significant risk factor to PDAC (Yadav *et al.*, 2011). To examine this, congenic wild-type ($Atf3^{+/+}$) and $Atf3^{-/-}$ mice were exposed to recurrent saline (vehicle control) or cerulein I.P injections (250 μg/kg) twice daily for 14 days and allowed to recover 7 days following the last injection. Body weights were measured throughout the experimental time period, and at 3 and 7 days following the last injection. Wild-type CIP-treated mice showed significant decreases in body weight compared to wild-type saline mice from days 8 to 17, before weight was restored by day 21 (p<0.05; **Figure 3.10**). Similar analysis in $Atf3^{-/-}$ mice did not reveal significant decreases in body weight relative to wild type saline treated mice.

To assess tissue damage, saline and CIP-treated pancreatic tissues were assessed by histology 7 days following cessation of CIP. H&E staining demonstrated increased fibrosis and inflammatory infiltration in wild-type CIP-treated mice compared to $Atf3^{-/-}$

Day 1
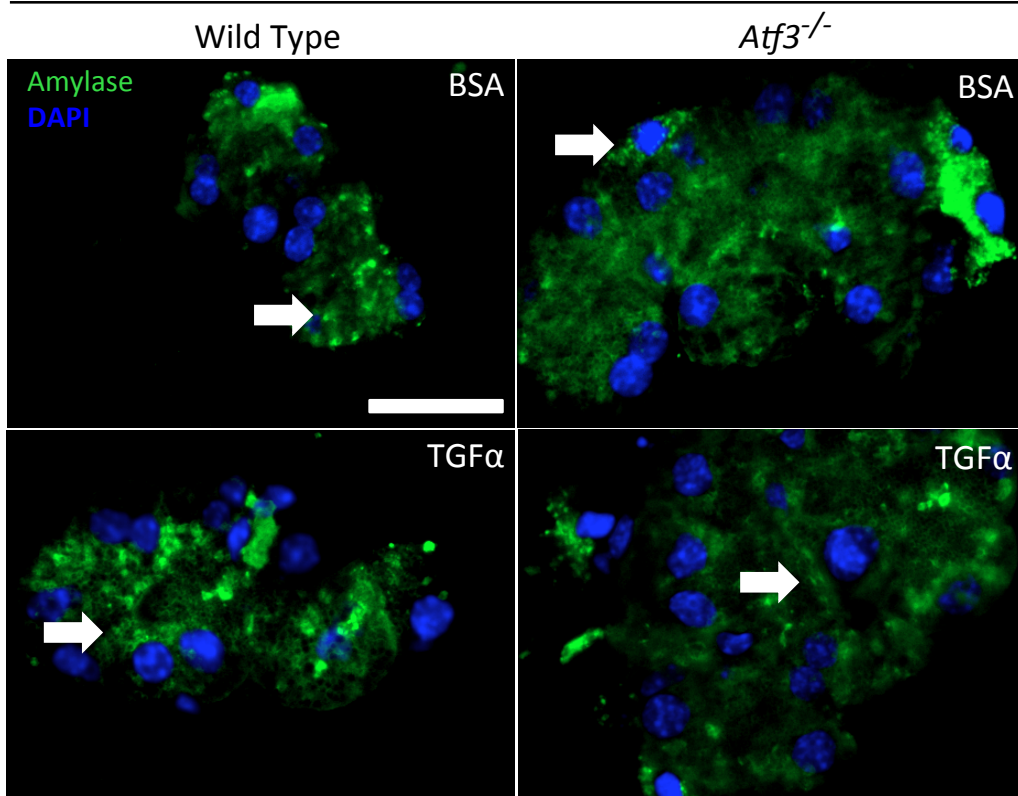
Wild Type	*Atf3*^{-/-}

Day 3
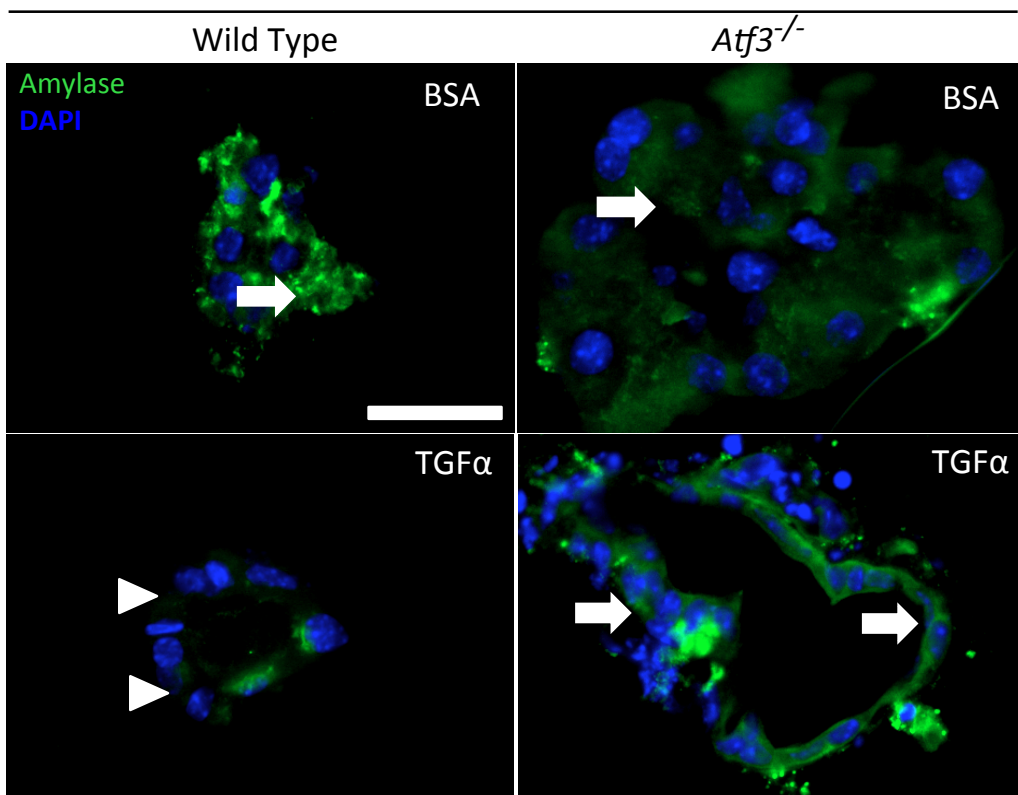
Figure 3.9 *Atf3*^{-/-} acini maintain amylase expression in cyst structures.

Immunofluorescence staining for amylase in BSA and TGFα-treated wild-type and *Atf3*^{-/-} primary acinar cells. Amylase staining is observed in BSA and TGFα-treated cells at day 1 (arrows). Staining is mostly absent in wild-type TGFα-treated cells by day 3 (arrow heads), but remained detectable in *Atf3*^{-/-} acini (arrows) suggesting maintenance of the acinar phenotype in *Atf3*^{-/-} cells (n=3). Scale bars = 25 μm.
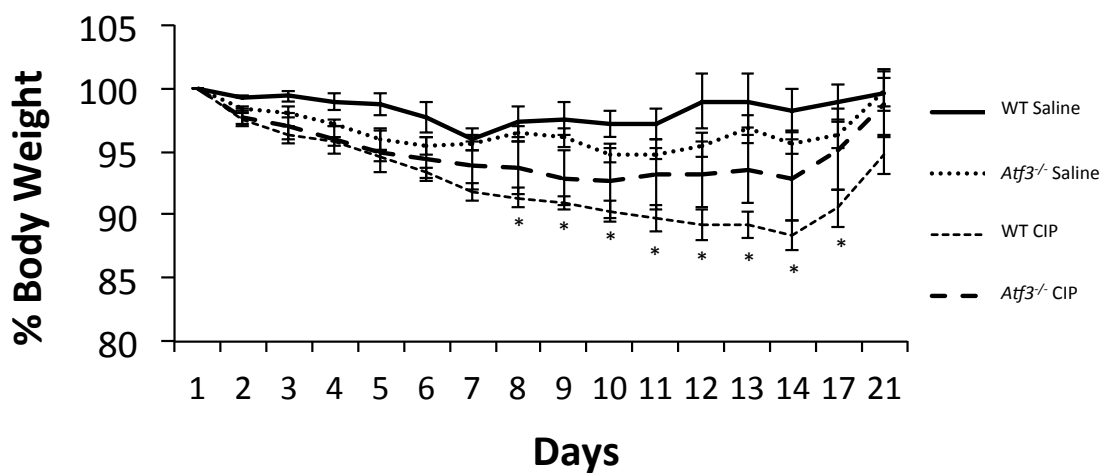
Figure 3.10 Wild-type mice show decreased body weight during recurrent pancreatitis. Chronic pancreatic injury was induced in wild-type (WT) and *Atf3*$^{-/-}$ mice by recurrent cerulein (CIP) injections (250 µg/kg body weight) twice daily for 14 days. Mice recovered for 7 days before sacrifice. Analysis of body weights over the injection period, as well as 3 and 7 days following cessation of CIP, indicates that presence of ATF3 during injury significantly decreases body weight from days 8 to 17 before weight restoration at day 21 (*p<0.05; n=5). Mean±SEM is shown.

A.
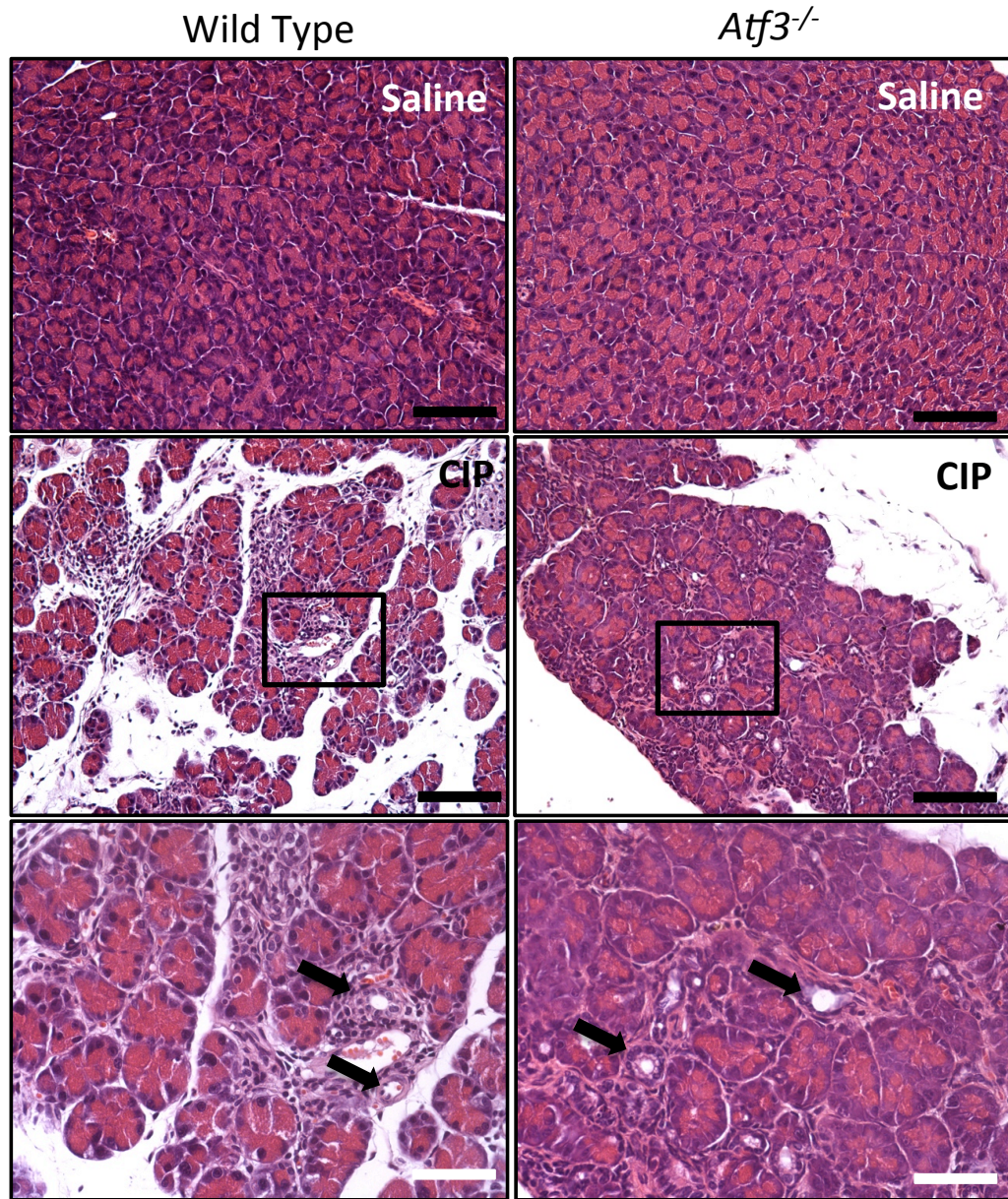
B.
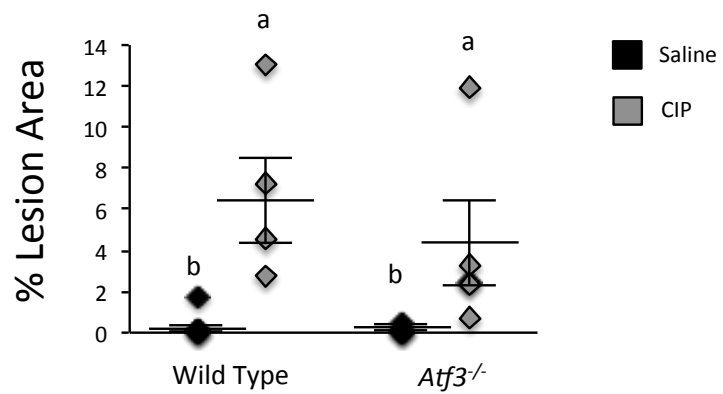
Figure 3.11 Recurrent pancreatic injury leads to damage in wild-type mice relative to *Atf3*^{-/-} mice. (A) Representative H&E histology of pancreatic tissue following chronic CIP-induced injury in wild-type and *Atf3*^{-/-} mice. Saline treated mice show no damage in response to treatment. Cerulein (CIP) treatment induced more damage (as evident by increased ADM and inflammation) in wild-type pancreata compared to *Atf3*^{-/-} CIP models. Black boxes indicate regions of higher magnification. Black scale bars = 100 μm. White scale bars = 50 μm. Representative of n=5. **(B)** Quantification for areas of damage and inflammation following chronic injury indicates significantly more lesion area relative to total tissue area following CIP treatment in both wild type and *Atf3*^{-/-} compared to saline (^{a}p>0.05), but no significant difference is observed between wild type and *Atf3*^{-/-} CIP treated samples (n=5). Mean±SEM is shown.

CIP-treated mice (**Figure 3.11A**). Lesion area (areas of damage and ADM) were assessed relative to total tissue area in wild type and *Atf3*^{-/-} saline and CIP treated mice. While there was a significant increase in percent lesion area in both the wild type and *Atf3*^{-/-} CIP models compared to saline (p>0.05), there was no significant different in lesion area between CIP treated samples (**Figure 3.11B**).

To provide further qualitative analysis of damage, trichrome staining was conducted on histological sections of pancreas tissues from wild-type and *Atf3*^{-/-} mice following chronic injury to assess tissue fibrosis. While damage is increased following CIP treatment in both genotypes, no overt differences in fibrosis were observed between wild-type and *Atf3*^{-/-} mice (**Figure 3.12**).

To determine if acinar cell de-differentiation was contributing to increased pancreatic tissue damage observed histologically, amylase protein levels were assessed by western blot. When analyzing individual samples, it appeared the majority of mice showed decreased amylase expression following chronic CIP treatment compared to saline, however no statistical significance was observed in both wild type and *Atf3*^{-/-} mice (p>0.05; **Figure 3.13)**.
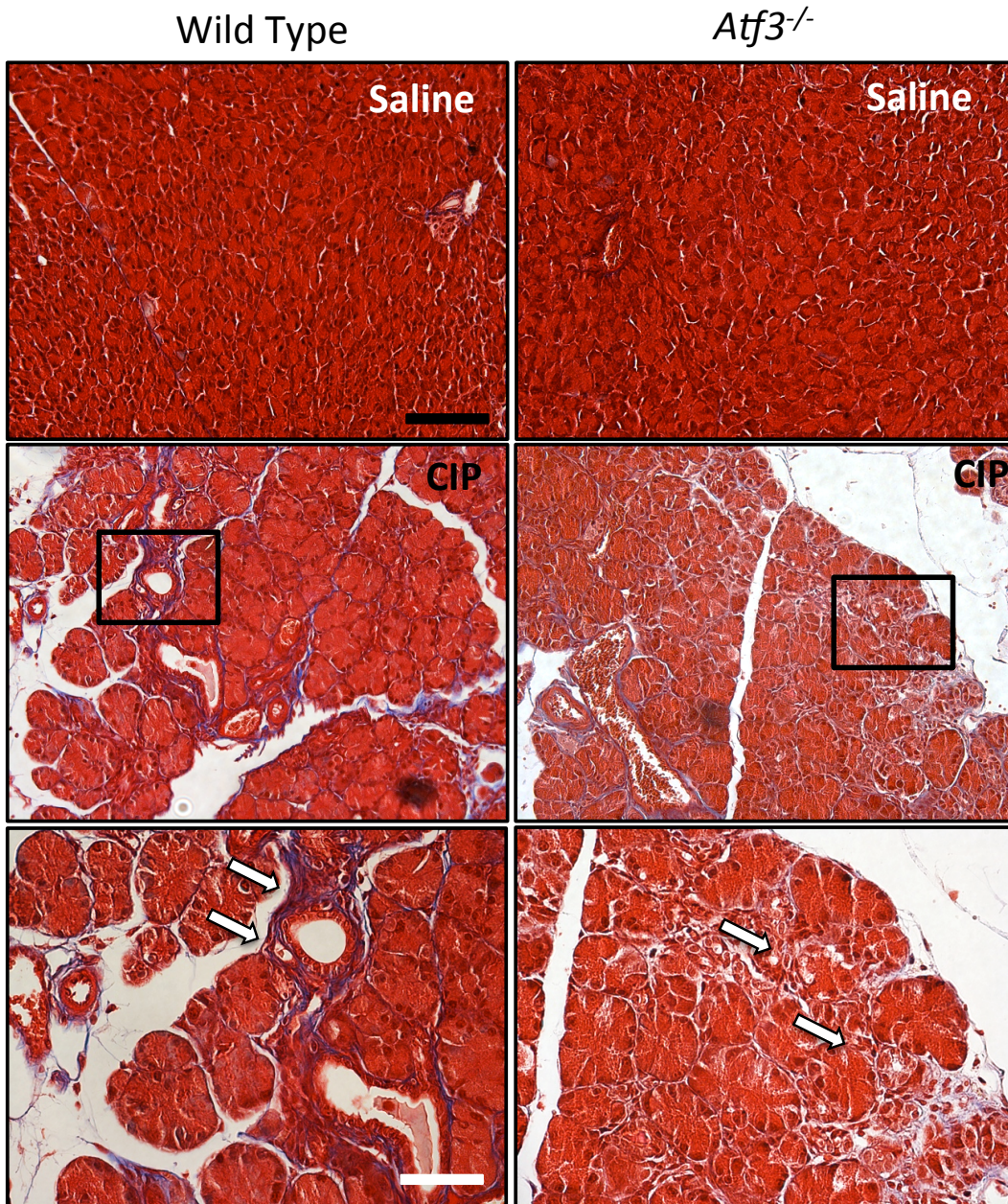
Figure 3.12 No differences in tissue fibrosis following chronic injury in wild type and *Atf3*^{-/-}. Representative Masson's trichrome staining following chronic pancreatic injury in wild type and *Atf3*^{-/-} mice. Cerulein treatment (CIP) increases damage relative to saline models (white arrows), however no differences in fibrotic tissue accumulation are observed between wild type and *Atf3*^{-/-} CIP treated mice. Black boxes indicate regions of higher magnification Black scale bars = 100 μm. White scale bars = 50 μm. Representative of n=5. Mean±SEM is shown.

A.
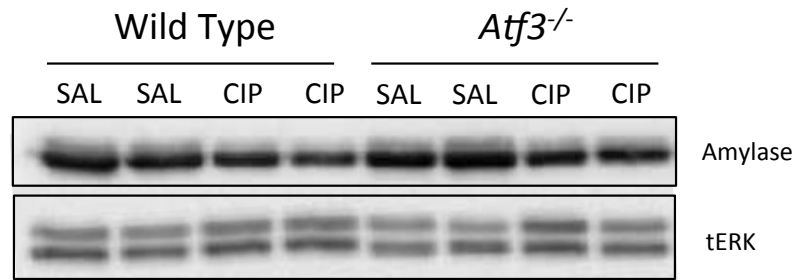
B.
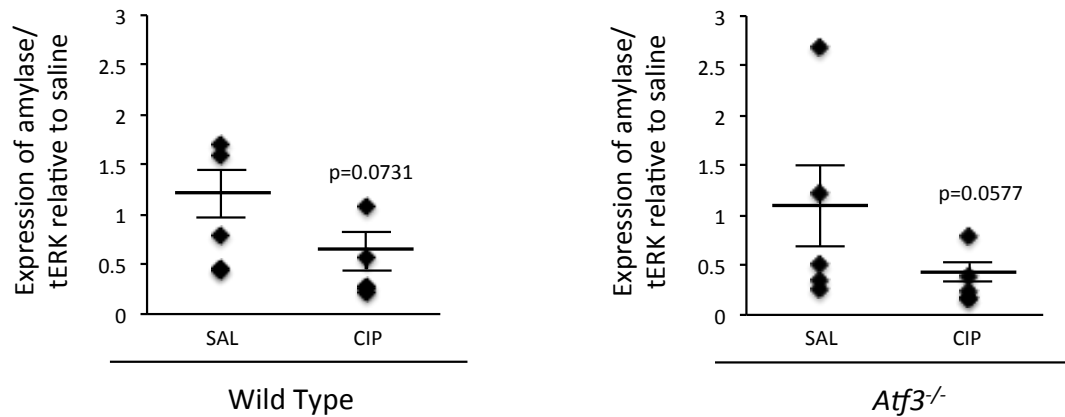
Figure 3.13 Cerulein treatment does not affect amylase expression in wild type and *Atf3-/-*. **(A)** Representative western blot analysis of amylase protein levels in pancreatic tissues 7 days following cessation of saline (SAL) or chronic cerulein (CIP). **(B)** Densitometry analysis of amylase relative to tERK following chronic injury indicates no statistical difference compared to saline in either wild type or *Atf3-/-* models ($p>0.05$; n=5). Mean±SEM is shown.

Chapter 4

4   Discussion and Conclusions

4.1   Overview

During acute pancreatic injury, acinar cells undergo de-differentiation as a protective mechanism to reduce further damage (Jensen *et al.*, 2005; Karki *et al.*, 2015). This de-differentiation process into a progenitor-like phenotype allows for regeneration of damaged cells, and repopulation of the exocrine pancreas (Murtaugh & Keefe, 2015; Karki *et al.*, 2015). In murine models with acute episodes of injury, complete regeneration occurs within 7 days (Grady *et al*., 1998; Yadav *et al*., 2011). However, if the cells are exposed to a continuous insult, the de-differentiation process becomes fixed, and cells cannot re-differentiate, therefore undergoing ADM (Logsdon & Ji., 2009; Morris *et al*., 2010). In this thesis, I show that ATF3 represses the acinar differentiation program at early time points following injury, and is required to maintain gene expression changes 72 hours following injury, when regeneration is occurring. Not only does ATF3 affect mRNA levels of genes required for mature acinar cell differentiation, but it also affects ADM-promoting pathways such as EGFR. Loss of *Atf3* reduced expression of EGFR pathway regulators (*Egfr, Mek1*) following injury relative to saline, which may explain the reduced damage, and decreased formation of ADM in primary acinar cultures that are evident in the absence of *Atf3*.

Patients with chronic pancreatitis are more susceptible to developing PDAC; therefore exploring *Atf3* following chronic insult was necessary (Yadav & Lowenfels, 2013). Loss of *Atf3* resulted in decreased inflammatory infiltration and damage following chronic injury. These findings provide evidence that ATF3 directs ADM development and worsens the pancreatic phenotype following injury. However, it is still important to determine whether *Atf3* is contributing to this worsened phenotype by increasing damage, or preventing the regenerative program.

4.2   ATF3 targets transcription factors required for ADM

Previous studies from our lab showed that following acute pancreatic injury, the loss of *Atf3* initially caused a worsened phenotype, with increased damage and fibrosis (Fazio *et al*., 2017). However, when comparing degree of regeneration at a later time point (72 hours), loss of *Atf3* promoted increased healthy acinar tissue and reduced incidences of damage, while wild-type mice showed increased ADM. The phenotypic changes that were evident histologically are explained by how the differentiation program is affected by insult. *Atf3* contributes to repression of the differentiation program through decreased expression of *Rbpjl* and *Nr5a2* (**Figure 3.1A; Figure 3.2**)*.* It is difficult to conclude whether the decreases in expression that are observed are due to direct ATF3-mediated transcriptional regulation. It may be that *Atf3* is re-activating the progenitor program, as seen through increases in expression of *Sox9* (**Figure 3.3)**, and that these cells decrease mature transcription factor expression because they are de-differentiating. However, recently published data from our lab suggests that ATF3 is directly affecting the mature acinar phenotype by repression of *Nr5a2*, *Rbpjl*, and *Mist1* gene expression (Fazio *et al*.,

2017). ChIP sequencing data suggests that *Atf3* accumulates on the promoter regions of

Nr5a2 and *Rbpjl,* suggesting an influence on the transcriptional programs that maintain

differentiated acinar cells. To conclusively demonstrate whether *Atf3* is affecting

transcription of these genes, determining what other proteins are binding with ATF3 to

the DNA is necessary. ATF3 can repress transcriptional programs by recruitment of

inhibitory HDACs to gene promoters (Kwon *et al.*, 2015). In line with this result, we

have shown that ATF3 recruits HDAC5 to the *Mist1* promoter, leading to repression, and

therefore downregulation of the mature acinar phenotype (Fazio *et al.,* 2017). Therefore,

ATF3 may be functioning in a similar manner to decrease expression of *Nr5a2* and *Rbpjl*.

As stated previously, it cannot be excluded that ATF3 directly upregulates the progenitor

and duct programs to promote ADM. Results from previous ChIP sequencing data

suggested that ATF3 increased expression of *Sox9* and *Krt19* through direct binding to

promoter regions (Fazio *et al.*, 2017). There is also evidence that ATF3 binds to and

represses expression of other pancreatic progenitor markers, such as *Pdx1* in β-cells (Jang

et al., 2001). This study showed that ATF3 could directly bind to promoters of pancreatic

progenitor factors. In acinar cells, we would expect ATF3 to promote progenitor gene

expression rather than repress progenitor gene expression as it does in β-cells. The

difference in ATF3's mechanism of action in β-cells compared to acinar cells may be due

to additional proteins, bound along with ATF3 in a transcriptional complex, that are

responsible for directing a decrease in expression. The mechanism by which ATF3 can

cause activation or repression of these factors remains to be determined. Since it is

known that ATF3 can regulate expression of progenitor genes (Jang, 2011), exploring

how ATF3 regulates expression of other progenitor and ductal cell factors, such as *Sox9*

and *Krt19*, will allow us to determine if *Atf3* is responsible for activating transcription of these factors. While changes to *Krt19* expression may be secondary to ATF3's effects, as *Sox9* can increase expression of this ductal marker (Murtaugh & Keefe, 2015), it is still worth exploring the transcriptional complexes that ATF3 is a part of which increase progenitor and ductal expression.

In addition to the role that ATF3 plays in regulating the acinar transcriptional program, it may also be forcing ADM through increased EGFR signalling, a known driver of ADM. Activation of EGFR by EGF and TGFα ligands has been shown in both *in vitro* and *in vivo* pancreatic injury models (Sandgren *et al.*, 1990; Means *et al.*, 2005). In murine models, upregulation of EGFR signalling through increased TGFα expression by a metallothionein-promoter indicates the necessity of this pathway in initiating ADM, and progressing to PDAC (Sandgren *et al*., 1990). As well, these changes are an acinar-specific event, as isolated primary pancreatic acinar cells show transformation to a ductal phenotype upon treatment with TGFα (Means *et al*., 2005). Previous work in our lab has shown that ATF3 has an effect on EGFR signalling, as Kyoto Encyclopedia of Genes and Genomes (KEGG) pathway analysis following RNA-sequencing shows that loss of ATF3 downregulates the expression of genes associated with EGF signalling following injury (Fazio *et al*., 2017). This is reflected by qRT-PCR analysis, which shows that *Egfr* is elevated in wild type and *Atf3*$^{-/-}$ models 4 hours following acute injury relative to saline, but remains elevated at 72 hours in only wild type models (**Figure 3.5A**). Since overexpression of EGFR is implicated in human PDAC cases (Fitzgerald *et al.*, 2015), it may be that ATF3 is initiating transcription of *Egfr* and *Mek1*, leading to overexpression

of these pathways, and potentially increased activation and ADM. The loss of *Atf3* may then be protective against EGFR-induced ADM, as it decreases transcription of EGFR.

ATF3 may also affect the EGFR pathway further downstream. Phosphorylated ERK proteins are responsible for activating transcription of various factors required to induce cell functions such as cell survival or proliferation. ERK has been implicated in activating transcription of NFκB and JUN (Chang *et al.*, 2003; Molina & Adjei, 2006; Roberts & Der, 2007), both proteins which are implicated in ATF3 signalling (Jiang *et al.*, 2004; Liang *et al.*, 2006; Kwon *et al.*, 2015). Therefore, pERK may be functioning as a feedback mechanism to further induce ATF3 transcription, which can then act together with NFkB and JUN to induce inflammation and proliferation, and therefore promote ADM. Analysis of this possibility would need to be explored further. A limitation to the current analysis is a lack of significance in pERK levels between genotypes due to insufficient n values (**Figure 3.6B**). I show that there may be association between EGFR-related genes (*Egfr and Mek1*) and ERK pathway activation, however to show that ERK activation is a direct result of EGFR signalling needs to be elucidated. Repeating this experiment with increased mice may provide more definitive data.

While the effects of ATF3 on EGFR-mediated ADM have been investigated in this study, to truly understand whether ATF3 is responsible for ADM, it would be necessary to analyze the effects of ATF3 on other ADM-promoting signalling pathways, such as Notch signaling. In combination with additional PDAC driving mutations, such as KRAS, Notch signaling accelerates the reprogramming process (Morris *et al.*, 2010). This indicates that differential expression of multiple developmental signalling pathways is implicated in cancer progression. Loss of ATF3 may therefore be not only decreasing

ADM through EGFR signalling, but through repression of inappropriately re-activated notch signalling. Analysis of downstream factors of Notch signalling between wild-type and *Atf3⁻/⁻* mouse tissue would elucidate this possibility.

4.3 ADM formation in primary acinar cells is affected by the loss of ATF3

The necessity of ATF3 as a driver of the ADM process was analyzed through primary acinar cultures. Treatment of wild-type and *Atf3⁻/⁻* acinar cells with TGFα forced acinar cell de-differentiation into cyst, tubular structures representative of ADMs (**Figure 3.7**). Interestingly, loss of ATF3 did not lead to decreased cyst formation as predicted. However, the structures that formed were not indicative of ADM, as these cells maintained expression of the mature acinar marker amylase. Differences in cyst formation may not have been observed due to overactive EGFR signalling in both wild type and *Atf3⁻/⁻*. As overexpression of EGFR activates ADM (Fitzgerald *et al*., 2015), it may be that the *Atf3⁻/⁻* acinar cultures were treated with a high concentration of TGFα, and that despite decreases in *Egfr* and *Mek1* expression implicated with a loss of *Atf3* (**Figure 3.4**), activation of this pathway was still able to initiate the ADM process. However, phenotypic ADMs did not form in *Atf3⁻/⁻* cultures, as these cells maintained an acinar phenotype, indicating there still is differential pathway activation (**Figure 3.9**). These cultures were only analyzed up to a 3 day time point. It is known that cyst structures of true ADMs are able to survive in culture for up to 14 days (Means *et al*., 2005). Therefore, these cultures should be analyzed at time points beyond what I have documented in this study. I would predict that *Atf3⁻/⁻* cysts would undergo apoptosis if

followed beyond a 3-day time point, while the wild type ADMs persist in culture for days following.

To determine the extent of how ATF3 affects ADM, additional pancreatic enzymes and markers of a mature acinar phenotype should be examined, such as β-catenin. It has been previously shown that maintenance of β-catenin signalling is necessary for blocking ADM, and is an important predictor of acinar cell fate and PDAC development (Morris *et al.*, 2010). If the loss of *Atf3* leads to maintained β-catenin, as indicated in our previous *in vivo* work (Fazio *et al.*, accepted), it provides further validation to the prediction that *Atf3* is implicated in ADM.

4.4 Increased damage in wild-type mice may be predictive of decreased ability to regenerate following injury

Chronic pancreatitis increases susceptibility to PDAC development (Yadav & Lowenfels, 2013). As ADM is a known precursor to PDAC development (Logsdon & Ji, 2009), identifying the role of ATF3 in mediating ADM following chronic injury is necessary. Our data shows that loss of ATF3 prevents loss of body weight from days 8 to 14 of injury, and up to 3 days into recovery (**Figure 3.10**). This suggests that ATF3 may contribute to increased pancreatic damage. As is evident histologically, loss of *Atf3* reduced inflammatory infiltration and damage, and decreased ADM. These assessments were completed 7 days following the final injection of cerulein. At the cessation of injury, pancreatic acinar cells will attempt to repair damage and undergo regeneration (Murtaugh & Keefe, 2015). Evidence of increased and maintained damage in wild-type mice during the regenerative period following chronic injury is of particular interest. This raises the question as to whether ATF3 expression contributes to increased ADM through

increasing damage, potentially through increased inflammation, or is blocking the regenerative process.

Increased damage observed with ADM is typically caused by an increased inflammatory response. Following injury, macrophages infiltrate the tissue immediately to try and mediate a tissue repair process (Deschênes-Simard *et al.*, 2013). However, continuous exposure to injury, such as chronic pancreatitis, will alter the immune program, and lead to pathogenic inflammatory injury. Loss of ATF3 may be decreasing the damage following chronic pancreatitis through its effects on NFκB. Interactions between ATF3 and NFκB inhibited inflammatory activity and reduced damage following acute kidney injury (Li *et al*., 2010; Kwon *et al*., 2015). It may be that in the case of chronic pancreatic injury, ATF3 interacts with a different transcriptional complex to instead activate NFκB, and promote the inflammatory response leading to increased damage. Another possibility is that loss of ATF3 decreases the damage phenotype by promoting a more differentiated, mature acinar phenotype, and therefore blocking inflammation and ADM. Previous results from our lab have shown that ATF3 represses *Mist1*, a factor known to reduce pancreatic defects and ADM following exposure to injury (Kowalik *et al.*, 2007; Karki *et al.*, 2015) . Along with decreased expression in *Nr5a2* (**Figure 3.2**), the loss of these pro-differentiation factors will sensitize acinar tissue to injury and allow for inflammation to persist, and can therefore activate fibrosis via pancreatic stellate cell activation (Murtaugh & Keefe, 2015). The potential that loss of ATF3 following chronic injury is protecting against increased damage would need to be investigated further.

An alternative possibility is that decreased damage is observed with the loss of ATF3 because of the ability of these cells to regenerate to a greater degree. Wild-type mice

show increased ADM following chronic injury, while the absence of ATF3 leads to a greater accumulation of healthy acinar tissue (**Figure 3.11**). The inability of wild-type acinar cells to regenerate may be because of ATF3's effects on signalling pathways required for regeneration to occur. Studies have shown that following injury, acinar cells are replaced by expansion of residual surviving cells, rather than neogenesis from a stem cell population (Murtaugh & Keefe, 2015). Regeneration is driven by the Notch signalling pathway (Siveke *et al.*, 2008; Murtaugh & Keefe, 2015). The Notch pathway is normally activated during embryonic development and regulates exocrine cell fate. However, it is expressed at low levels in adult pancreatic tissue, and only becomes re-activated during the regenerative phase of pancreatitis. Notch signalling will increase expression of RBPJ, driving acinar cell progenitor formation and decreasing ductal and islet differentiation. Maintenance of notch signalling for extended periods leads to inhibition of PTF1A-mediated acinar genes, such as *Mist1* and *Nr5a2*, and leads to decreased differentiation (Stanger & Hebrok, 2013; von Figura *et al.*, 2014; Karki *et al.*, 2015). ATF3 may be acting on Notch signalling to maintain its activation, allowing acinar cells to de-differentiate, in an attempt to undergo regeneration, but not re-differentiate to repopulate damaged areas. Increased notch signalling by ATF3 may therefore be sensitizing acinar cells to oncogenic transformation and promote ADM. Evidence of this occurring is clear in our *in vivo* genetic analysis following acute injury, as loss of *Atf3* shows a decreased ratio of *Rbpj/Rbpjl* expression following acute pancreatitis (**Figure 3.1B**). In addition to Notch activation, *Nr5a2* is required for normal acinar regeneration as this transcription factor drives terminal differentiation. Since *Atf3*

is implicated in decreasing expression of this factor (**Figure 3.2**), it may also be repressing regeneration by this mechanism.

The absence of *Atf3* following acute pancreatic injury also decreases expression of factors implicated in the EGFR pathway (*Egfr and Mek1*), and therefore may also be promoting regeneration by repressing ADM formation mediated by EGFR. ATF3 may be increasing damage following chronic CIP through maintenance of re-activated notch signalling, and increased EGFR activation. To confirm this, further experiments analyzing ATF3s effects on notch signalling, are necessary. Analysis of notch-activating ligands, Jagged-1,-2, and Delta-1 can be assessed to determine if there are differences between genotypes (Su *et al.*, 2006).

In acute models of ADM, we see that loss of ATF3 initially leads to increased damage, however these mice are able to recover to a greater extent compared to the wild-type. Based on these results, we would predict that with chronic pancreatitis, a loss of ATF3 would result in worse damage initially, but that these mice would recover quicker. In order to truly test this hypothesis, the recurrent injury experiment would be repeated with a cohort of mice assessed immediately following injury cessation to assess the differences in damage.

This study included limitations of both the *in-vivo* and *in-vitro* work. Due to insufficient n values for acute pancreatic mouse studies, differences between genders could not be assessed. Repeating these experiments with increased n values, and an even group of both male and female mice will allow for this analysis. Difficulties in culturing primary acinar cells beyond 3 days provided limitations to the *in-vitro* work. Assessment of cyst

development and potential cyst size differences between wild type and *Atf3*$^{-/-}$ cells could not be completed since primary acinar cells were not viable beyond 3 days-post isolation. Alterations to the acinar isolation protocol will perhaps increase viability of these cells and allow for extended analysis. Additionally, we cannot conclude that the pancreatic phenotype we observe is not due to the loss of ATF3 in pancreatic stellate cells and macrophages. Development of a pancreas specific ATF3 knock-out will eliminate the potential of these off-target effects.

4.5 Future Directions and Conclusions

To establish the mechanism by which *Atf3* is regulating genetic expression of acinar, progenitor, and duct factors, further analysis must be performed. Determining other transcriptional targets that are bound with *Atf3* in a transcriptional complex will elude to the roles it plays to either activate or repress transcription. Performing co-immunoprecipitation assays will allow for resolution of co-binding activating or repressing factors. Understanding these complexes will allow for a more targeted approach to reduce ADM formation.

The role that *Atf3* plays in the EGFR signalling pathway has been minimally explored. To fully understand why loss of *Atf3* still resulted in cyst formation, treatment of acinar cultures with varying concentrations of TGFα is important. It will be necessary to perform a concentration gradient of TGFα, and then analyze EGFR activation in both wild type and *Atf3*$^{-/-}$ primary cultures. Repeating treatment with the newly determined concentrations and assessing cyst formation for days following treatment will provide a greater insight into this process. To further provide support to ATF3's role in EGFR signalling, ADM, and finally PDAC formation, introducing a loss of *Atf3* with a mutated

KRAS gene is necessary. Currently, mouse lines are being developed that contain an inducible *KRAS^{G12D}* driven by an acinar specific *Ptf1a*-cre. Exploring the role that *Atf3* plays in ADM development with a KRAS mutation will allow for a better understanding in how it may be increasing susceptibility to PDAC.

Finally, as alluded to in the discussion, it is unknown whether *Atf3* is implicated in increasing damage or repressing regeneration following chronic injury. Repeating the experiment and analyzing the mice at time points immediately following cessation of injury will allow for us to definitively conclude ATF3's role in either promoting damage or blocking regeneration.

In conclusion, this study identifies *Atf3* as potential regulator of ADM. ATF3 may be driving this process through either affecting the acinar genetic program to promote progenitor and ductal cell formation, through increased EGFR signalling, or both (**Figure 4.1**). While ATF3 is not necessary for cyst formation, as evident in primary acinar cultures, it is implicated in the ADM process since loss of *Atf3* results in maintained mature acinar marker expression (amylase). To determine the role of ATF3 in driving the ADM process following chronic injury, and therefore potentially increasing susceptibility to PDAC, analyzing how loss of *Atf3* reduces ADM, through either decreasing damage or increasing regenerative capacity, is necessary (**Figure 4.1**). Further studies to elucidate the mechanism of genetic regulations in the pancreas will provide insight as to how ATF3 may be targeted for either diagnostic or therapeutic purposes.
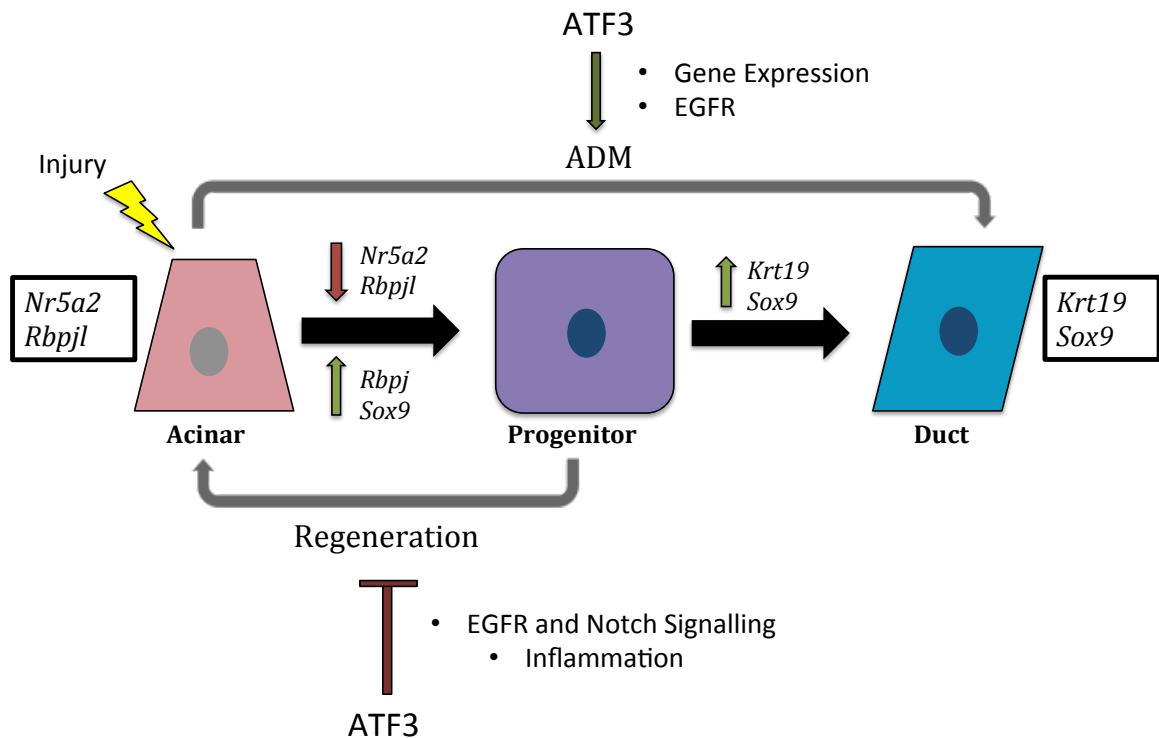
Figure 4.1 ATF3 promotes acinar-to-duct cell metaplasia by affecting the acinar genetic program and inhibiting pancreatic regeneration following injury. When the pancreas is exposed to injury, it will attempt to regenerate and repopulate damaged acinar cells. However, ATF3 may be blocking this regenerative process and instead promote acinar-to-duct cell metaplasia (ADM) by affecting the acinar genetic program and increasing EGFR signalling. Regeneration may be inhibited by ATF3s effects on EGFR and Notch signalling, as well as inflammation.

References

Aghdassi AA, Mayerle J, Christochowitz S, Weiss FU, Sendler M & Lerch MM (2011). Animal models for investigating chronic pancreatitis. *Fibrogenesis Tissue Repair* **4,** 26.

Alahari S, Mehmood R, Johnson CL & Pin CL (2011). The absence of MIST1 leads to increased ethanol sensitivity and decreased activity of the unfolded protein response in mouse pancreatic acinar cells. *PLoS One* **6,** e28863.

Allen-Jennings AE, Hartman MG, Kociba GJ & Hai T (2001). The roles of ATF3 in glucose homeostasis. A transgenic mouse model with liver dysfunction and defects in endocrine pancreas. *J Biol Chem* **276,** 29507–29514.

Ardito CM et al. (2012). EGF receptor is required for KRAS-induced pancreatic tumorigenesis. *Cancer Cell* **22,** 304–317.

Bandyopadhyay S, Wang Y, Zhan R, Pai SK, Watabe M, Iiizumi M, Furuta E, Mohinta S, Liu W, Hirota S, Hosobe S, Tsukada T, Miura K, Takano Y, Saito K, Commes T, Piquemal D, Hai T & Watabe K (2006). The Tumor Metastasis Suppressor Gene Drg-1 Down-regulates the Expression of Activating Transcription Factor 3 in Prostate Cancer. *Cancer Res* **66,** 11983–11990.

Bernales S (2006). Intracellular Signaling by the Unfolded Protein Response. **22,** 487–508.

Calfon M, Zeng H, Urano F, Till JH, Hubbard SR, Harding HP, Clark SG & Ron D (2002). IRE1 couples endoplasmic reticulum load to secretory capacity by processing the XBP-1 mRNA. *Nature* **415,** 92–96.

Chang F, Steelman LS, Lee JT, Shelton JG, Navolanic PM, Blalock WL, Franklin RA & McCubrey JA (2003). Signal transduction mediated by the Ras/Raf/MEK/ERK pathway from cytokine receptors to transcription factors: potential targeting for

therapeutic intervention. *Leukemia* **17,** 1263–1293.

Cid-Arregui A & Juarez V (2015). Perspectives in the treatment of pancreatic adenocarcinoma. *World J Gastroenterol* **21,** 9297–9316.

Cláudio N, Dalet A, Gatti E & Pierre P (2013). Mapping the crossroads of immune activation and cellular stress response pathways. *EMBO J* **32,** 1214–1224.

Deschênes-Simard X, Mizukami Y & Bardeesy N (2013). Macrophages in pancreatic cancer: starting things off on the wrong track. *J Cell Biol* **202,** 403–405.

Ebine K et al. (2016). Slug inhibits pancreatic cancer initiation by blocking Kras-induced acinar-ductal metaplasia. *Sci Rep* **6,** 29133.

Eser S, Schnieke A, Schneider G & Saur D (2014). Oncogenic KRAS signalling in pancreatic cancer. *Br J Cancer* **111,** 817–822.

von Figura G, Morris JP, Wright CVE & Hebrok M (2014). Nr5a2 maintains acinar cell differentiation and constrains oncogenic Kras-mediated pancreatic neoplastic initiation. *Gut* **63,** 656–664.

Fazio EN, Young CC, Toma J, Levy M, Berger KB, Johnson CL, Mehmood R, Swan P, Chu A, Cregan SP, Dilworth JF, Howlett CJ, Pin CL. (2017). Activating Transcription Factor 3 is a key transcriptional regulator during exocrine pancreatic injury. *Molecular Biology of the Cell*. Accepted. doi:10.1091/mbc.E17-04-0254

Fitzgerald TL, Lertpiriyapong K, Cocco L, Martelli AM, Libra M, Candido S, Montalto G, Cervello M, Steelman L, Abrams SL & McCubrey JA (2015). Roles of EGFR and KRAS and their downstream signaling pathways in pancreatic cancer and pancreatic cancer stem cells. *Adv Biol Regul* **59,** 65–81.

Fu L & Kilberg MS (2013). Elevated cJUN expression and an ATF/CRE site within the ATF3 promoter contribute to activation of ATF3 transcription by the amino acid response. *Physiol Genomics* **45,** 127–137.

Gifford JB, Huang W, Zeleniak AE, Hindoyan A, Wu H, Donahue TR & Hill R (2016). Expression of GRP78, Master Regulator of the Unfolded Protein Response, Increases Chemoresistance in Pancreatic Ductal Adenocarcinoma. *Mol Cancer Ther* **15,** 1043–1052.

Gilchrist M, Henderson WR, Clark AE, Simmons RM, Ye X, Smith KD & Aderem A (2008). Activating transcription factor 3 is a negative regulator of allergic pulmonary inflammation. *J Exp Med* **205,** 2349–2357.

Grady T, Mah'Moud M, Otani T, Rhee S, Lerch MM & Gorelick FS (1998). Zymogen proteolysis within the pancreatic acinar cell is associated with cellular injury. *Am J Physiol Gastrointest Liver Physiol* **275,** G1010-1017.

Guerra C & Barbacid M (2013). Genetically engineered mouse models of pancreatic adenocarcinoma. *Mol Oncol* **7,** 232–247.

Hai T & Hartman MG (2001). The molecular biology and nomenclature of the activating transcription factor/cAMP responsive element binding family of transcription factors: activating transcription factor proteins and homeostasis. *Gene* **273,** 1–11.

Harding HP, Zhang Y, Bertolotti A, Zeng H & Ron D (2000). Perk Is Essential for Translational Regulation and Cell Survival during the Unfolded Protein Response. *Mol Cell* **5,** 897–904.

Hartman MG, Lu D, Kim M-L, Kociba GJ, Shukri T, Buteau J, Wang X, Frankel WL, Guttridge D, Prentki M, Grey ST, Ron D & Hai T (2004). Role for activating transcription factor 3 in stress-induced beta-cell apoptosis. *Mol Cell Biol* **24,** 5721–5732.

Hashimoto Y, Zhang C, Kawauchi J, Imoto I, Adachi MT, Inazawa J, Amagasa T, Hai T & Kitajima S (2002). An alternatively spliced isoform of transcriptional repressor ATF3 and its induction by stress stimuli. *Nucleic Acids Res* **30,** 2398–2406.

Haze K, Yoshida H, Yanagi H, Yura T & Mori K (1999). Mammalian transcription factor ATF6 is synthesized as a transmembrane protein and activated by proteolysis in

response to endoplasmic reticulum stress. *Mol Biol Cell* **10,** 3787–3799.

Hess DA, Humphrey SE, Ishibashi J, Damsz B, Lee A-H, Glimcher LH & Konieczny SF (2011). Extensive pancreas regeneration following acinar-specific disruption of Xbp1 in mice. *Gastroenterology* **141,** 1463–1472.

Houbracken I, de Waele E, Lardon J, Ling Z, Heimberg H, Rooman I & Bouwens L (2016). Lineage Tracing Evidence for Transdifferentiation of Acinar to Duct Cells and Plasticity of Human Pancreas. *Gastroenterology* **141,** 731–741.e4.

Huang X, Li X & Guo B (2008). KLF6 induces apoptosis in prostate cancer cells through up-regulation of ATF3. *J Biol Chem* **283,** 29795–29801.

Iwawaki T, Akai R & Kohno K (2010). IRE1α Disruption Causes Histological Abnormality of Exocrine Tissues, Increase of Blood Glucose Level, and Decrease of Serum Immunoglobulin Level ed. Polymenis M. *PLoS One* **5,** e13052.

James CG, Woods A, Underhill TM & Beier F (2006). The transcription factor ATF3 is upregulated during chondrocyte differentiation and represses cyclin D1 and A gene transcription. *BMC Mol Biol* **7,** 30.

Jang MK (2011). ATF3 represses PDX-1 expression in pancreatic β-cells. *Biochem Biophys Res Commun* **412,** 385–390.

Jang MK, Kim CH, Seong JK & Jung MH (2012). ATF3 inhibits adipocyte differentiation of 3T3-L1 cells. *Biochem Biophys Res Commun* **421,** 38–43.

Janz M, Hummel M, Truss M, Wollert-Wulf B, Mathas S, Jöhrens K, Hagemeier C, Bommert K, Stein H, Dörken B & Bargou RC (2006). Classical Hodgkin lymphoma is characterized by high constitutive expression of activating transcription factor 3 (ATF3), which promotes viability of Hodgkin/Reed-Sternberg cells. *Blood* **107,** 2536–2539.

Jennings RE, Berry AA, Strutt JP, Gerrard DT & Hanley NA (2015). Human pancreas development. *Development* **142,** 3126–3137.

Jensen JN, Cameron E, Garay MVR, Starkey TW, Gianani R & Jensen J (2005). Recapitulation of elements of embryonic development in adult mouse pancreatic regeneration. *Gastroenterology* **128,** 728–741.

Ji B, Chen X, Misek DE, Kuick R, Hanash S, Ernst S, Najarian R & Logsdon CD (2003). Pancreatic gene expression during the initiation of acute pancreatitis: identification of EGR-1 as a key regulator. *Physiol Genomics* **14,** 59–72.

Jiang H-Y, Wek SA, McGrath BC, Lu D, Hai T, Harding HP, Wang X, Ron D, Cavener DR & Wek RC (2004). Activating transcription factor 3 is integral to the eukaryotic initiation factor 2 kinase stress response. *Mol Cell Biol* **24,** 1365–1377.

Jiang X, Kim K-J, Ha T & Lee S-H (2016). Potential Dual Role of Activating Transcription Factor 3 in Colorectal Cancer. *Anticancer Res* **36,** 509–516.

Johnson CL, Kowalik AS, Rajakumar N & Pin CL (2004). Mist1 is necessary for the establishment of granule organization in serous exocrine cells of the gastrointestinal tract. *Mech Dev* **121,** 261–272.

Johnson CL, Peat JM, Volante SN, Wang R, McLean CA & Pin CL (2012). Activation of protein kinase Cδ leads to increased pancreatic acinar cell dedifferentiation in the absence of MIST1. *J Pathol* **228,** 351–365.

Karki A, Humphrey SE, Steele RE, Hess DA, Taparowsky EJ & Konieczny SF (2015). Silencing Mist1 Gene Expression Is Essential for Recovery from Acute Pancreatitis. *PLoS One* **10,** e0145724.

Kopp JL, von Figura G, Mayes E, Liu F-F, Dubois CL, Morris JP, Pan FC, Akiyama H, Wright CVE, Jensen K, Hebrok M & Sander M (2012). Identification of Sox9-dependent acinar-to-ductal reprogramming as the principal mechanism for initiation of pancreatic ductal adenocarcinoma. *Cancer Cell* **22,** 737–750.

Kowalik AS, Johnson CL, Chadi SA, Weston JY, Fazio EN & Pin CL (2007). Mice lacking the transcription factor Mist1 exhibit an altered stress response and increased sensitivity to caerulein-induced pancreatitis. *Am J Physiol Gastrointest*

Liver Physiol **292,** G1123-32.

Krah NM, De La O J-P, Swift GH, Hoang CQ, Willet SG, Chen Pan F, Cash GM, Bronner MP, Wright CV, MacDonald RJ & Murtaugh LC (2015). The acinar differentiation determinant PTF1A inhibits initiation of pancreatic ductal adenocarcinoma. *Elife* **4,** e07125.

Kubisch CH, Sans MD, Arumugam T, Ernst SA, Williams JA & Logsdon CD (2006). Early activation of endoplasmic reticulum stress is associated with arginine-induced acute pancreatitis. *Am J Physiol Gastrointest Liver Physiol* **291,** G238-45.

Kwon J-W, Kwon H-K, Shin H-J, Choi Y-M, Anwar MA & Choi S (2015). Activating transcription factor 3 represses inflammatory responses by binding to the p65 subunit of NF-κB. *Sci Rep* **5,** 14470.

Lee K, Tirasophon W, Shen X, Michalak M, Prywes R, Okada T, Yoshida H, Mori K & Kaufman RJ (2002). IRE1-mediated unconventional mRNA splicing and S2P-mediated ATF6 cleavage merge to regulate XBP1 in signaling the unfolded protein response. *Genes Dev* **16,** 452–466.

Li H-F, Cheng C-F, Liao W-J, Lin H & Yang R-B (2010). ATF3-mediated epigenetic regulation protects against acute kidney injury. *J Am Soc Nephrol* **21,** 1003–1013.

Liang G, Wolfgang CD, Chen BP, Chen TH & Hai T (1996). ATF3 gene. Genomic organization, promoter, and regulation. *J Biol Chem* **271,** 1695–1701.

Liang S-H, Zhang W, McGrath BC, Zhang P & Cavener DR (2006). PERK (eIF2alpha kinase) is required to activate the stress-activated MAPKs and induce the expression of immediate-early genes upon disruption of ER calcium homoeostasis. *Biochem J* **393,** 201–209.

Liou G-Y, Döppler H, Braun UB, Panayiotou R, Scotti Buzhardt M, Radisky DC, Crawford HC, Fields AP, Murray NR, Wang QJ, Leitges M & Storz P (2015). Protein kinase D1 drives pancreatic acinar cell reprogramming and progression to intraepithelial neoplasia. *Nat Commun* **6,** 6200.

Logsdon CD & Ji B (2009). Ras activity in acinar cells links chronic pancreatitis and pancreatic cancer. *Clin Gastroenterol Hepatol* **7,** S40-3.

Logsdon CD & Ji B (2013). The role of protein synthesis and digestive enzymes in acinar cell injury. *Nat Rev Gastroenterol Hepatol* **10,** 362–370.

Logsdon CD & Lu W (2016). The Significance of Ras Activity in Pancreatic Cancer Initiation. *Int J Biol Sci* **12,** 338–346.

Lowenfels AB (2006). Epidemiology and risk factors for pancreatic cancer. *Best Pract Res Clin Gastroenterol* **20,** 197–209.

Lu D, Wolfgang CD & Hai T (2006). Activating transcription factor 3, a stress-inducible gene, suppresses Ras-stimulated tumorigenesis. *J Biol Chem* **281,** 10473–10481.

Lugea A (2011). Adaptive Unfolded Protein Response Attenuates Alcohol-Induced Pancreatic Damage. *Gastroenterology* **140,** 987–997.e8.

Maas NL & Diehl JA (2015). Molecular pathways: the PERKs and pitfalls of targeting the unfolded protein response in cancer. *Clin Cancer Res* **21,** 675–679.

Martinelli P, Madriles F, Cañamero M, Pau ECS, Pozo N Del, Guerra C & Real FX (2016). The acinar regulator Gata6 suppresses KrasG12V-driven pancreatic tumorigenesis in mice. *Gut* **65,** 476–486.

Masui T, Swift GH, Deering T, Shen C, Coats WS, Long Q, Elsässer H, Magnuson MA & MacDonald RJ (2010). Replacement of Rbpj With Rbpjl in the PTF1 Complex Controls the Final Maturation of Pancreatic Acinar Cells. *Gastroenterology* **139,** 270–280.

Means AL, Meszoely IM, Suzuki K, Miyamoto Y, Rustgi AK, Coffey RJ, Wright CVE, Stoffers DA & Leach SD (2005). Pancreatic epithelial plasticity mediated by acinar cell transdifferentiation and generation of nestin-positive intermediates. *Development* **132,** 3767–3776.

Miyatsuka T (2006). Persistent expression of PDX-1 in the pancreas causes acinar-to-ductal metaplasia through Stat3 activation. *Genes Dev* **20,** 1435–1440.

Molina JR & Adjei AA (2006). The Ras/Raf/MAPK Pathway. *J Thorac Oncol* **1,** 7–9.

Morris JP, Cano DA, Sekine S, Wang SC & Hebrok M (2010). Beta-catenin blocks Kras-dependent reprogramming of acini into pancreatic cancer precursor lesions in mice. *J Clin Invest* **120,** 508–520.

Murtaugh LC & Keefe MD (2015). Regeneration and repair of the exocrine pancreas. *Annu Rev Physiol* **77,** 229–249.

Namba T & Kodama R (2015). Avarol induces apoptosis in pancreatic ductal adenocarcinoma cells by activating PERK-eIF2α-CHOP signaling. *Mar Drugs* **13,** 2376–2389.

Papachristou GI, Clermont G, Sharma A, Yadav D & Whitcomb DC (2007). Risk and markers of severe acute pancreatitis. *Gastroenterol Clin North Am* **36,** 277–96, viii.

Pelzer AE, Bektic J, Haag P, Berger AP, Pycha A, Schäfer G, Rogatsch H, Horninger W, Bartsch G & Klocker H (2006). The Expression of Transcription Factor Activating Transcription Factor 3 in the Human Prostate and its Regulation by Androgen in Prostate Cancer. *J Urol* **175,** 1517–1522.

Pin CL, Bonvissuto AC & Konieczny SF (2000). Mist1 expression is a common link among serous exocrine cells exhibiting regulated exocytosis. *Anat Rec* **259,** 157–167.

Pin CL, Rukstalis JM, Johnson C & Konieczny SF (2001). The bHLH transcription factor Mist1 is required to maintain exocrine pancreas cell organization and acinar cell identity. *J Cell Biol* **155,** 519–530.

Piper K, Brickwood S, Turnpenny LW, Cameron IT, Ball SG, Wilson DI & Hanley NA (2004). Beta cell differentiation during early human pancreas development. *J Endocrinol* **181,** 11–23.

Prevot P-P, Simion A, Grimont A, Colletti M, Khalaileh A, Van den Steen G, Sempoux C, Xu X, Roelants V, Hald J, Bertrand L, Heimberg H, Konieczny SF, Dor Y, Lemaigre FP & Jacquemin P (2012). Role of the ductal transcription factors HNF6 and Sox9 in pancreatic acinar-to-ductal metaplasia. *Gut* **61,** 1723–1732.

Reichert M & Rustgi AK (2011). Pancreatic ductal cells in development, regeneration, and neoplasia. *J Clin Invest* **121,** 4572–4578.

Roberts GH (2015). Pancreatitis. *J Contin Educ Top Issues* **17,** 4–11.

Roberts PJ & Der CJ (2007). Targeting the Raf-MEK-ERK mitogen-activated protein kinase cascade for the treatment of cancer. *Oncogene* **26,** 3291–3310.

Ron D, Bertolotti A, Zhang Y, Hendershot LM & Harding HP (2000). Dynamic interaction of BiP and ER stress transducers in the unfolded-proteinresponse. *Nat Cell Biol* **2,** 326–332.

Rooman I & Real FX (2012). Pancreatic ductal adenocarcinoma and acinar cells: a matter of differentiation and development? *Gut* **61,** 449 LP-458.

Sah RP, Garg SK, Dixit AK, Dudeja V, Dawra RK & Saluja AK (2014). Endoplasmic reticulum stress is chronically activated in chronic pancreatitis. *J Biol Chem* **289,** 27551–27561.

Sandgren EP, Luetteke NC, Palmiter RD, Brinster RL & Lee DC (1990). Overexpression of TGF? in transgenic mice: Induction of epithelial hyperplasia, pancreatic metaplasia, and carcinoma of the breast. *Cell* **61,** 1121–1135.

Scotti ML, Smith KE, Butler AM, Calcagno SR, Crawford HC, Leitges M, Fields AP & Murray NR (2012). Protein kinase C iota regulates pancreatic acinar-to-ductal metaplasia. *PLoS One* **7,** e30509.

Shi G (2009). Loss of the Acinar-Restricted Transcription Factor Mist1 Accelerates Kras-Induced Pancreatic Intraepithelial Neoplasia. *Gastroenterology* **136,** 1368–1378.

Shi G, DiRenzo D, Qu C, Barney D, Miley D & Konieczny SF (2013). Maintenance of acinar cell organization is critical to preventing Kras-induced acinar-ductal metaplasia. *Oncogene* **32,** 1950–1958.

Siegel RL, Miller KD & Jemal A (2017). Cancer statistics, 2017. *CA Cancer J Clin* **67,** 7–30.

Siveke JT, Lubeseder–Martellato C, Lee M, Mazur PK, Nakhai H, Radtke F & Schmid RM (2008). Notch Signaling Is Required for Exocrine Regeneration After Acute Pancreatitis. *Gastroenterology* **134,** 544–555.e3.

Stanger BZ & Hebrok M (2013). Control of Cell Identity in Pancreas Development and Regeneration. *Gastroenterology* **144,** 1170–1179.

Storz P (2017). Acinar cell plasticity and development of pancreatic ductal adenocarcinoma. *Nat Rev Gastroenterol Hepatol* **14,** 296–304.

SU Y, BUCHLER P, GAZDHAR A, GIESE N, REBER H, HINES O, GIESE T, BUCHLER M & FRIESS H (2006). Pancreatic Regeneration in Chronic Pancreatitis Requires Activation of the Notch Signaling Pathway. *J Gastrointest Surg* **10,** 1230–1242.

Syed V, Mukherjee K, Lyons-Weiler J, Lau K-M, Mashima T, Tsuruo T & Ho S (2005). Identification of ATF-3, caveolin-1, DLC-1, and NM23-H2 as putative antitumorigenic, progesterone-regulated genes for ovarian cancer cells by gene profiling. *Oncogene* **24,** 1774–1787.

Thompson MR, Xu D & Williams BRG (2009). ATF3 transcription factor and its emerging roles in immunity and cancer. *J Mol Med (Berl)* **87,** 1053–1060.

Wang Z, Xu D, Ding H-F, Kim J, Zhang J, Hai T & Yan C (2015). Loss of ATF3 promotes Akt activation and prostate cancer development in a Pten knockout mouse model. *Oncogene* **34,** 4975–4984.

Wang Z & Yan C (2015). Emerging roles of ATF3 in the suppression of prostate cancer.

Mol Cell Oncol **3,** e1010948.

Wei J, Gaut JR & Hendershot LM (1995). In vitro dissociation of BiP-peptide complexes requires a conformational change in BiP after ATP binding but does not require ATP hydrolysis. *J Biol Chem* **270,** 26677–26682.

Whitcomb DC (2010). Genetic Aspects of Pancreatitis. *Annu Rev Med* **61,** 413–424.

Williams JA (2010). Regulation of acinar cell function in the pancreas. *Curr Opin Gastroenterol* **26,** 478–483.

Wu J & Kaufman RJ (2006). From acute ER stress to physiological roles of the Unfolded Protein Response. *Cell Death Differ* **13,** 374–384.

Wu J, Rutkowski DT, Dubois M, Swathirajan J, Saunders T, Wang J, Song B, Yau GD-Y & Kaufman RJ (2007). ATF6α Optimizes Long-Term Endoplasmic Reticulum Function to Protect Cells from Chronic Stress. *Dev Cell* **13,** 351–364.

Yadav D & Lowenfels A (2013). The Epidemiology of Pancreatitis and Pancreatic Cancer. *Gastroenterology* **144,** 1252–1261.

Yadav D, Timmons L, Benson JT, Dierkhising RA & Chari ST (2011). Incidence, Prevalence, and Survival of Chronic Pancreatitis: A Population-Based Study. *Am J Gastroenterol* **106,** 2192–2199.

Yewale C, Baradia D, Vhora I, Patil S & Misra A (2013). Epidermal growth factor receptor targeting in cancer: A review of trends and strategies. *Biomaterials* **34,** 8690–8707.

Zhang Y, Liu T, Meyer CA, Eeckhoute J, Johnson DS, Bernstein BE, Nusbaum C, Myers RM, Brown M, Li W & Liu XS (2008). Model-based analysis of ChIP-Seq (MACS). *Genome Biol* **9,** R137.

Zhao J, Li X, Guo M, Yu J & Yan C (2016). The common stress responsive transcription factor ATF3 binds genomic sites enriched with p300 and H3K27ac for

transcriptional regulation. *BMC Genomics* **17,** 335.

Appendices
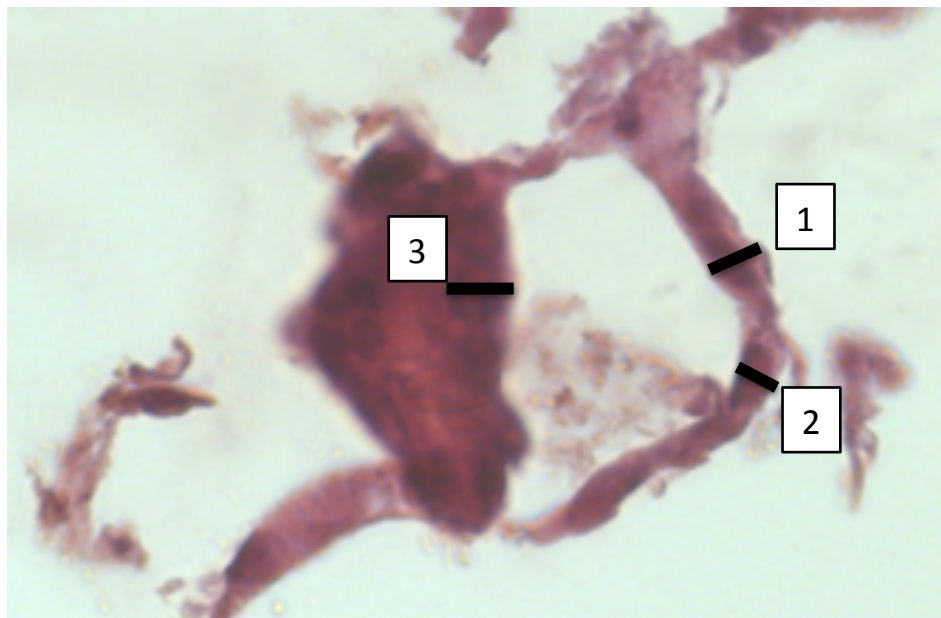
Appendix 1. Representative analysis of cell thickness

Representative analysis of cell thickness in reference to Figure 9. Using Image J software, 3 points around the cyst were measured across the length of the nuclei to determine the thickness of the cells composing the cyst. An average of 3 distinct points per cyst was recorded.

Curriculum Vitae

Name: Jelena Toma

Post-secondary Education and Degrees:

The University of Western Ontario   2015 – present

- Masters of Science
- Physiology and Pharmacology

The University of Western Ontario   2011 - 2015

- Bachelor of Medical Science
- Honors Specialization in Physiology
- Minor in Pharmacology

Honours and Awards:

2017	- Best poster in Cancer Biology Research at Physiology and Pharmacology Research Day
2016	- Ontario Graduate Scholarship Recipient
	- Poster Presentation at American Pancreatic Association Conference
2015	- Scholarship holder for Cancer Research and Technology Transfer Program
2011-2015	- Dean's Honour List
2011	- Western Scholarship of Distinction

Related Work Experience:

University of Western Ontario: Physiology and Pharmacology Department

Physiology Lab (3130Z)   September 2015-present

- Teaching Assistant
    - Provide guidance on how to approach scientific experiments

- o Encourage independent thinking for hypothesis and protocol development
- o Evaluate scientific papers and presentations

University of Western Ontario: Physiology and Pharmacology Department

Victoria Research Labs – Children's Health Research Institute   May – August 2015

- Lab Research Assistant
  - o Supervisor: Dr. Christopher Pin
  - o Learned various staining techniques
  - o Assisted in genotyping of various mouse lines

University of Western Ontario: Physiology and Pharmacology Department

May – July 2014

- Lab Research Assistant
  - o Supervisor: Dr. Nica Borradaile
  - o Assisted in western blotting and cell culturing
  - o Learned techniques for histological analysis

Publications:

1. Fazio E, Young C, **Toma J**, Levy M, Berger K, Johnson C, Mehmood R, Swan P, Chu A, Cregan S, Dilworth J, Howlett C, Pin CL. (2017) Activating Transcription Factor 3 is a key transcriptional regulator during exocrine pancreatic injury. *Molecular Biology of the Cell*. (Accepted). doi:10.1091/mbc.E17-04-0254

2. Pang DKT, Nong Z, Sutherland BG, Sawyez CG, Robson DL, **Toma J**, Pickering GJ, Borradaile NM. (2016) Niacin promotes revascularization and recovery of limb function in diet-induced obese mice with peripheral ischemia. *Pharmacology Research & Perspectives*, 4(3), e00233. http://doi.org/10.1002/prp2.233

3. Hughes-Large JM, Pang DKT, Robson DL, Chan P, **Toma J,** Borradaile NM. (2014) Niacin receptor activation improves human microvascular endothelial cell angiogenic function during lipotoxicity. *Atherosclerosis*, 237(2):696-704. doi:10.1016/j.atherosclerosis.2014.10.090